NeuroImage 195 (2019) 409–432

Contents lists available at ScienceDirect

NeuroImage

journal homepage: www.elsevier.com/locate/neuroimage

Mediation analysis of triple networks revealed functional feature of mindfulness from real-time fMRI neurofeedback

Hyun-Chul Kim [a], Marion Tegethoff [b], Gunther Meinlschmidt [c,d,e], Esther Stalujanis [b,e], Angelo Belardi [b], Sungman Jo [a], Juhyeon Lee [a], Dong-Youl Kim [a], Seung-Schik Yoo [f], Jong-Hwan Lee [a,*]

[a] Department of Brain and Cognitive Engineering, Korea University, Seoul, South Korea
[b] Division of Clinical Psychology and Psychiatry, Department of Psychology, University of Basel, Basel, Switzerland
[c] Division of Clinical Psychology and Epidemiology, Department of Psychology, University of Basel, Basel, Switzerland
[d] Department of Psychosomatic Medicine, University Hospital Basel and University of Basel, Basel, Switzerland
[e] Division of Clinical Psychology and Cognitive Behavioral Therapy, International Psychoanalytic University, Berlin, Germany
[f] Department of Radiology, Brigham and Women's Hospital, Harvard Medical School, Boston, MA, USA

ARTICLE INFO

Keywords:
Central executive network
Contemplative science
Default-mode network
Functional connectivity
Functional magnetic resonance imaging
Mediation analysis
Mindfulness
Real-time fMRI neurofeedback
Salience network

ABSTRACT

The triple networks, namely the default-mode network (DMN), the central executive network (CEN), and the salience network (SN), play crucial roles in disorders of the brain, as well as in basic neuroscientific processes such as mindfulness. However, currently, there is no consensus on the underlying functional features of the triple networks associated with mindfulness. In this study, we tested the hypothesis that (a) the partial regression coefficient (i.e., slope): from the SN to the DMN, mediated by the CEN, would be one of the potential mindfulness features in the real-time functional magnetic resonance imaging (rtfMRI) neurofeedback (NF) setting, and (b) this slope level may be enhanced by rtfMRI-NF training. Sixty healthy mindfulness-naïve males participated in an MRI session consisting of two non-rtfMRI-runs, followed by two rtfMRI-NF runs and one transfer run. Once the regions-of-interest of each of the triple networks were defined using the non-rtfMRI-runs, the slope level was calculated by mediation analysis and used as neurofeedback information, in the form of a thermometer bar, to assist with participant mindfulness during the rtfMRI-NF runs. The participants were asked to increase the level of the thermometer bar while deploying a mindfulness strategy, which consisted of focusing attention on the physical sensations of breathing. rtfMRI-NF training was conducted as part of a randomized controlled trial design, in which participants were randomly assigned to either an experimental group or a control group. The participants in the experimental group received contingent neurofeedback information, which was obtained from their own brain signals, whereas the participants in the control group received non-contingent neurofeedback information that originated from matched participants in the experimental group. Our results indicated that the slope level from the SN to the DMN, mediated by the CEN, was associated with mindfulness score (rtfMRI-NF runs: $r = 0.53$, $p = 0.007$; p-value was corrected from 10,000 random permutations) and with task-performance feedback score (rtfMRI-NF run: $r = 0.61$, $p = 0.001$) in the experimental group only. In addition, during the rtfMRI-NF runs the level of the partial regression coefficient feature was substantially increased in the experimental group compared to the control group ($p < 0.05$ from the paired t-test; the p-value was corrected from 10,000 random permutations). To the best of our knowledge, this is the first study to demonstrate a partial regression coefficient feature of mindfulness in the rtfMRI-NF setting obtained by triple network mediation analysis, as well as the possibility of enhancement of the partial regression coefficient feature by rtfMRI-NF training.

* Corresponding author. Department of Brain and Cognitive Engineering Korea University, Anam-ro 145, Seongbuk-gu, Seoul, 02841, Republic of Korea.
E-mail address: jonghwan_lee@korea.ac.kr (J.-H. Lee).

https://doi.org/10.1016/j.neuroimage.2019.03.066
Received 8 June 2018; Received in revised form 5 March 2019; Accepted 27 March 2019
Available online 3 April 2019

1. Introduction

Three prominent, functionally-connected large-scale networks, comprised of the default-mode network (DMN), the central executive network (CEN), and the salience network (SN), are collectively known as the triple network (Menon, 2011). These triple networks reflect typical developmental changes, including those of emotional dysfunction, aberrant saliency mapping, and cognitive dysfunction, which are characteristics of a range of mental and neurological disorders such as anxiety disorders, depressive disorders, autism, schizophrenia, Alzheimer's disease, and frontotemporal dementia (Menon, 2011; Touroutoglou et al., 2015; Uddin et al., 2011; Young et al., 2017). The DMN includes the posterior cingulate cortex (PCC) and the ventromedial prefrontal cortex (vmPFC) and is known for its role in self-related (i.e., internally directed) perception (Brewer and Garrison, 2014; Brewer et al., 2011; Fair et al., 2008; Mooneyham et al., 2016; Sheline et al., 2009; Sridharan et al., 2008; Uddin, 2015). On the other hand, the CEN includes the posterior parietal cortex and the dorsolateral prefrontal cortex (dlPFC) and is known for its function in goal-oriented (i.e., externally directed) cognition (Beaty et al., 2015; Christoff et al., 2016; Mooneyham et al., 2016; Sridharan et al., 2008; Uddin, 2015). In contrast, the SN includes the dorsal anterior insular cortex (dAIC) and the dorsal anterior cingulate cortex (dACC) and is known as the hub of interoceptive perception (Barrett and Simmons, 2015; Mooneyham et al., 2016). In addition, the SN influences signals in the DMN and the CEN causally and dynamically (Mooneyham et al., 2016; Uddin, 2015).

In recent years, mindfulness has gained increasing interest across a variety of research fields because of its potential benefits, including improvements in executive function, emotional regulation, working memory, and vigilance. Furthermore, mindfulness has pre-clinical benefits applicable to a broad range of mental disorders such as addictions, anxiety disorders, and depressive disorders (Baer, 2003; Diamond and Lee, 2011; Dunne, 2018; Hofmann et al., 2010; Miller et al., 1995; Mooneyham et al., 2016; Morgan, 2003; Wang et al., 2018; Weick et al., 2008; Zeidan et al., 2010). Interestingly, a particular set of brain regions involved with mindfulness appears to lie within the triple network (Brewer et al., 2011; Dickenson et al., 2013; Doll et al., 2016; Hasenkamp and Barsalou, 2012; Lutz et al., 2015; Mooneyham et al., 2016). Accordingly, recent neuroimaging studies on mindfulness have focused on changes in functional connectivity (FC) within and/or between the triple networks (Bilevicius et al., 2018; Brewer et al., 2011; Creswell et al., 2016; Doll et al., 2016; Hasenkamp and Barsalou, 2012; King et al., 2016; Lim et al., 2018; Lutz et al., 2015; Marusak et al., 2018; Mooneyham et al., 2016; Peters et al., 2016; Shaurya Prakash et al., 2012; Taren et al., 2017). Two findings consistently emerge from these previous studies: first, an increase of FC within the DMN (e.g., between the posterior DMN, including the PCC, and the anterior DMN, including the vmPFC), potentially because of an increase in self-referential processing (Hasenkamp and Barsalou, 2012; Mooneyham et al., 2016; Wells et al., 2013), and, second, an increase in FC between the SN and the CEN, potentially because of conscious executive processing (associated with the CEN) of moment-to-moment interoceptive perception (associated with the SN) (Brewer et al., 2011; Hasenkamp and Barsalou, 2012; Mooneyham et al., 2016; Seeley et al., 2007). Other than these findings, likely because of the diversity of mindfulness practices and methodological designs, there has been no unequivocal consensus on the FC features of mindfulness (Doll et al., 2015; Froeliger et al., 2012; Kilpatrick et al., 2011; Lutz et al., 2015; Mooneyham et al., 2016).

Early pioneering work on real-time fMRI-based neurofeedback (rtfMRI-NF) has shown that participants can learn volitional control over their own blood-oxygenation-level-dependent (BOLD) signals (deCharms et al., 2005; Posse et al., 2003; Weiskopf et al., 2003, 2004a, 2004b; Yoo et al., 2004; Yoo and Jolesz, 2002). Since then, a number of studies have demonstrated the utility of rtfMRI-NF successfully. In addition, the applicability of rtfMRI-NF has been extensively discussed in several recent review papers covering a broad range of its basic neuroscientific aspects and pre-clinical applications (Ruiz et al., 2014; Sitaram et al., 2017; Sulzer et al., 2013a; Thibault et al., 2018; Weiskopf, 2012), its use as a tool for clinical interventions (Kim and Birbaumer, 2014; Linden and Turner, 2016; Stoeckel et al., 2014), and advanced techniques such as decoding-based neurofeedback (Watanabe et al., 2017). Furthermore, increasing effort has been made to enhance the level of mindfulness using the rtfMRI-NF method applying the strategy of focusing attention on the physical sensations of breathing. The neurofeedback information (or signal) provided to participants is calculated by using the BOLD intensities from the PCC that are associated with self-referential processing. Moreover, it has been reported that PCC activation is significantly lower in experienced meditators than non-meditators (Brewer and Garrison, 2014; Garrison et al., 2013). However, a single brain region such as the PCC may be limited in its ability to account for the neuronal underpinnings of complex cognitive processes, including mindfulness under rtfMRI-NF conditions (Garrison et al., 2013; Mooneyham et al., 2016). Instead, information from multiple hubs or the FC of networks of brain regions such as the triple network enables the neuronal underpinnings of mindfulness (Garrison et al., 2013; Mooneyham et al., 2016).

To the best of our knowledge, this is the first study to propose a rtfMRI-NF-based training approach for mindfulness by employing mediation analysis using the triple network to estimate neurofeedback information. To this end, mindfulness-naïve males were recruited to perform rtfMRI-NF-based mindfulness training using the strategy of focusing attention on the physical sensations of breathing (Brewer et al., 2011; Garrison et al., 2013; Meinlschmidt et al., 2016). We expected that (i) this mindfulness strategy would evoke activation in the SN, which is closely linked to visceromotor interoceptive perception (Barrett and Simmons, 2015; Mooneyham et al., 2016; Uddin, 2015) and (ii) the mindfulness status would be reflected in the self-referential processing of the DMN (Brewer and Garrison, 2014; Mooneyham et al., 2016; Uddin, 2015). In addition, the CEN, which is in charge of conscious executive processing (Mooneyham et al., 2016; Seeley et al., 2007), would also be expected to be involved in rtfMRI-NF-based mindfulness because participants watched neurofeedback information to evaluate their performance with respect to mindfulness.

More specifically, since participants were initiating a mindfulness strategy (i.e., focusing on the sensation of breathing) in a self-paced manner, the strategy was expected to affect the interoceptive perception of the SN. This was expected to be reflected as an inherent mindfulness status via the self-referential processing of the DMN. Thus, the BOLD signal in the SN would be expected to be an independent variable and the BOLD signal in the DMN a dependent variable. The anterior insula has been known to play a causal role in switching between the CEN and DMN, and the CEN and DMN would undergo competitive interactions to mediate between the external and internal worlds, respectively, depending on task paradigms and stimulus conditions (Bressler and Menon, 2010). The CEN would mediate the processes of interoceptive perception as indicated by the thermometer bar (i.e., between the SN and CEN; external conscious processing) and consequent self-referential processing (i.e., between the CEN and DMN; internal conscious processing). Thus, the BOLD signal in the CEN was adopted as a possible mediator in the mediation analysis. The frontoparietal control system (i.e., CEN in our study) has indeed been reported to be flexible hubs that regulate distributed systems across the sensorimotor and limbic (i.e., interoceptive perception in our study) according to the current task goals being processed by the brain (i.e., mindfulness), in which this control system has been active during mindfulness meditation (Cole et al., 2014). Thus, we hypothesized that (a) the partial regression coefficient (i.e., slope): from the SN to the DMN, mediated by the CEN, would be one of the potential features of mindfulness in the mediation analysis framework, and (b) this feature of mindfulness would be enhanced by rtfMRI-NF-based mindfulness training. rtfMRI-NF training was conducted as part of a randomized controlled trial design, which included an experimental group (subjects receiving contingent, real, neurofeedback information) and a control group (subjects receiving non-contingent

neurofeedback information from matched subjects in the experimental group).

2. Materials and methods

2.1. Overall study protocol

The data presented in this study were collected within a randomized controlled trial, which was registered at ClinicalTrials.gov (Identifier: NCT03148678; https://clinicaltrials.gov/ct2/show/NCT03148678). The Institutional Review Board of Korea University approved the entire study protocol, and participants provided written informed consent. All participants were recruited from one site (Korea University) where an MRI session was performed, and another site (University of Basel) managed all the logistics required to perform ambulatory training sessions with the recruited participants. Fig. 1a illustrates the overall study procedure along with the time intervals between sessions and the number of included/excluded participants. The detailed information is described in the following subsections.

2.1.1. Telephone interview

Volunteers were recruited from across the university campus using flyers, over the internet, and by word-of-mouth. Interested volunteers were screened for eligibility by telephone interview. Those who met our inclusion criteria (i.e., right handedness, no history of neurological or mental disorders, no previous experience with mindfulness meditation, and being smartphone users) were invited to a face-to-face interview.

2.1.2. Face-to-face interview

First, we reviewed the inclusion criteria for the invited volunteers using the Edinburgh Handedness Inventory (EHI) (Oldfield, 1971) and Patient Health Questionnaire (PHQ) (Spitzer et al., 1999). Also, we collected sociodemographic and self-report information on psychological measures including the Big Five Inventory-10 (BFI-10) (Rammstedt and John, 2007), Perceived Stress Scale (PSS) (Cohen et al., 1983; Lee et al., 2012a), Mindful Attention Awareness Scale (MAAS) (Brown and Ryan, 2003; Jeon et al., 2007), and the Visual Analog scale for Stress perception (VAS). Then, we informed participants regarding the study protocol in more detail, including (a) the mindfulness strategy (i.e., attention

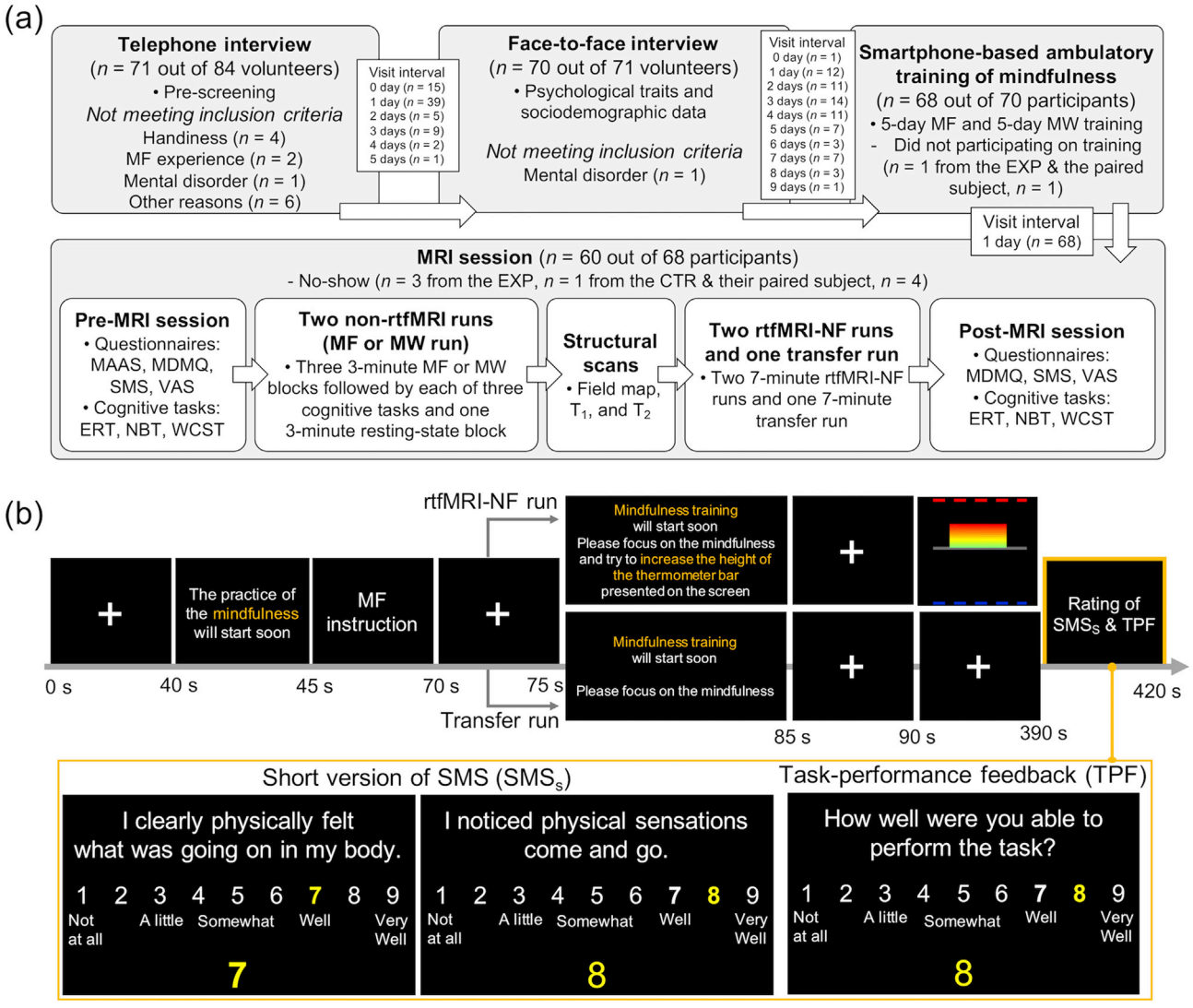

Fig. 1. (a) The overall study protocol including time intervals between sessions and number of participants included/excluded from the screened participants. (b) Task paradigm for the rtfMRI-NF run and the transfer run. See the "***Overall study protocol***" and "***Two real-time fMRI neurofeedback runs and one transfer run: online analysis***" subsection in the Methods section for details. The mindfulness instruction is described in Table 1. ERT, Emotion Recognition Task; MAAS, Mindful Attention Awareness Scale; MDMQ, Multidimensional Mood State Questionnaire; MF, mindfulness; MW, mind-wandering; NBT, *n*-back task (i.e., 3-back); non-rtfMRI, non-real-time fMRI; SMS, State Mindfulness Scale; VAS, Visual Analog scale for Stress perception; WCST, Wisconsin Card Sorting Test.

focused on the physical sensations of breathing), the mind-wandering strategy (i.e., connecting thoughts as they wish), and the resting-state strategy (Table 1), (b) how to perform the smartphone-based ambulatory training sessions during the next 10 consecutive days, (c) three cognitive tasks, including (i) the *n*-back task (NBT; $n = 3$), consisting of both digits (i.e., 0 to 9) and letters (i.e., *a* to *z*) (Smith and Jonides, 1997), (ii) a facial Emotion Recognition Task (ERT) (Lee et al., 2013), and (iii) the Wisconsin Card Sorting Test (WCST) as a cognitive control test (Grant; Berg, 1948; Monchi et al., 2001), as well as (d) the experimental procedures of the MRI session, which included two non-real-time fMRI (non-rtfMRI) runs, featuring mindfulness and mind-wandering, followed by two rtfMRI-NF runs and one transfer run.

2.1.3. Smartphone-based ambulatory training session

On each of the next 10 consecutive days following the face-to-face interview, an email was sent at 8 a.m. to each participant with a day-specific hyperlink that expired at 3 a.m. the following day. Participants were required to perform their ambulatory training within this time-frame and received a reminder email at 8 p.m. if they had not done so by then. During the ambulatory training session, the participants were asked to apply the mindfulness strategy for 5 days and the mind-wandering strategy for the other 5 days in a counter-balanced order (i.e., one strategy per day, alternating; please see the Supplementary Material section, "***Smartphone-based ambulatory training sessions***"). Participants were asked to initiate the daily ambulatory training using their assigned identification and personal codes that were created and given to them on the face-to-face interview day. Participants responded to the Multidimensional Mood State Questionnaire (or the MDMQ, with scales measuring good–bad, awake–tired, and calm–nervous mood; also known as *Multidimensionaler Befindlichkeitsfragebogen*, MDBF, in German) (Steyer et al., 1994, 1997), the short version of the State Mindfulness Scale (SMS_S) with two questions (Q8 and Q14; Fig. 1b) selected from the original version of the SMS (Tanay and Bernstein, 2013), and the VAS to measure their stress level. The Enterprise Feedback Suite Survey 10.0 (Questback GmbH, Berlin, Germany) was used to build the smartphone-based ambulatory training session with text instructions incorporating the mindfulness and mind-wandering strategies and the collection of questionnaire data, as well as automated invitational and reminder emails to participants.

2.1.4. MRI session

On the MRI experiment day, the participants answered several questionnaires, including the MAAS, MDMQ, SMS, and VAS. Then, the participants were briefed regarding the three cognitive tasks (i.e., ERT, NBT, and WCST). The participants conducted these tasks and, then, were loaded into the MRI scanner in a supine position to acquire MRI data in the following order: two non-real-time fMRI (non-rtfMRI) runs, a field-map, T_1-weighted and T_2-weighted anatomical images, and two rtfMRI-NF runs, followed by one transfer fMRI run (Fig. 1a). One non-rtfMRI run consisted of three 3-min blocks of mindfulness each followed by one 3-min block for each of the three cognitive tasks. There was also one 3-min resting-state block pseudo-randomly positioned between the three mindfulness-cognitive task blocks. The other non-rtfMRI run was the same, except that the mind-wandering rather than the mindfulness strategy was performed. The order of the two non-rtfMRI runs was counter-balanced and the SMS_S/TPF scores of each of the mindfulness and mind-wandering blocks were obtained. A white cross was fixed in the center of the screen for 30 s between consecutive blocks.

Fig. 1b illustrates the task paradigm of the two rtfMRI-NF runs and the one transfer run. During the 300 s neurofeedback period (i.e., from 90 s to 390 s) of each of the two rtfMRI-NF runs, the participants were informed that the height of the thermometer bar with a red-green-blue color scheme would correspond to their level of mindfulness. In addition, they were asked to increase and to maintain the height of the bar while employing the mindfulness strategy. Participants were informed that the current bar represented changes in their brain activity that had taken place approximately 50 s earlier. This lag of approximately 50 s was comprised of a 43.2 s temporal window (1.44 s/volume × 30 volumes) to conduct a mediation analysis and an additional 6 s from the hemodynamic response delay to the peak. This window size for mediation analysis in a sliding window framework was determined based on a previous report, in which a window size of 44 s provided a good tradeoff between the ability to resolve the dynamics and the quality of the correlation coefficient estimate used to quantify the dynamic functional connectivity (Allen et al., 2014).

After the neurofeedback period, a 30 s rating period was given to the participants to evaluate their mindfulness scores (i.e., SMS_S) and task-performance feedback (i.e., TPF) scores using a fiber-optic response pad (Current Design, Philadelphia, PA; www.curdes.com), which was placed in their right hand. MR-compatible binocular goggles (NordicNeuroLab, Bergen, Norway) were used to provide visual stimuli. During the 300 s period of the subsequent transfer run, a white cross was displayed in the center of a black screen for participants to fixate on, and participants were asked to deploy their learned strategy from the rtfMRI-NF runs to enhance their level of mindfulness without the thermometer bar. Then, a 30 s rating period was given to the participants to evaluate their mindfulness score and task-performance feedback score. Electroencephalography (EEG) data were also acquired simultaneously with fMRI. During the debriefing session that followed the MRI session (i.e., the post-MRI period), the participants replied to a battery of questionnaires (i.e., the MDMQ, SMS, and VAS) and again performed the three cognitive tasks (i.e., the ERT, NBT, and WCST) as in the pre-MRI period.

Table 1
Instructions for mindfulness, mind-wandering, and resting-state conditions.

Condition	Instruction
Mindfulness[a]	*Please pay attention to the physical sensation of your breath wherever you feel it most strongly in your body.* *Follow the natural and spontaneous movement of your breath, not trying to change it in any way. Simply pay attention to it.* *If you find that your attention has wandered to something else, gently but firmly bring it back to the physical sensation of your breath.* *Please keep your eyes open.*
Mind-wandering[b]	*Please think about whatever comes to mind and go wherever your mind takes you.* *Follow your thoughts as they arise and let your mind wander, not trying to force your thoughts in any specific direction.* *If you find that a new thought appears, simply allow your attention to shift to this new thought.* *Please keep your eyes open.*
Resting-state[c]	*Please relax and lie still in the scanner while remaining calm and awake.* *Please keep your eyes open.*

[a] Text was adapted from (Brewer et al., 2011; Garrison et al., 2013; Meinlschmidt et al., 2016).
[b] Text was adapted and extended from (Dickenson et al., 2013).
[c] Text was adapted from (Patriat et al., 2013).

2.2. Participants

Sixty right-handed, healthy male volunteers (mean ± standard deviation (STD); age = 25.1 ± 2.9 years) participated in this study. Each participant was randomly assigned to either the experimental or the control group based on a block randomization method and each experimental subject was paired with one control subject (see details in the "***Counterbalancing the task paradigm and randomization procedure to allocate participants to either the experimental or control group***" section of the Supplementary Materials). The participants were blinded to the group assignment and were informed about only the experimental paradigm and the tasks to deploy in the MRI session. All the participants were subject to the non-rtfMRI runs, followed by the rtfMRI-NF runs and one transfer run. The participants in the experimental group were given contingent neurofeedback information derived from their own brain signals, whereas the participants in the control group were given non-

contingent neurofeedback information, which originated from their paired subject in the experimental group.

2.3. Imaging parameters

A 3-T Siemens Tim-Trio scanner with a 12-channel head coil (Erlangen, Germany) was used to acquire the MRI data. The standard gradient-echo echo-planar-imaging (EPI) pulse sequence was used for fMRI data acquisition with the following parameters: multiband factor of two using in-plane multiband GeneRalized Autocalibrating Partial Parallel Acquisition acceleration (or, GRAPPA 2); time of repetition (TR) = 1440 ms; time of echo (TE) = 30 ms; field-of-view (FoV) = 192 × 192 mm^2; voxel size = 3 × 3 × 3 mm^3; flip angle (FA) = 71°; 50 axial slices with no gap. The 3D magnetization-prepared rapid gradient-echo (MPRAGE) pulse sequence was used to acquire a T_1-weighted image (TR/TE = 1900/2.52 ms; FoV = 256 × 256 mm^2; voxel size = 1 × 1 × 1 mm^3; FA = 9°; 176 sagittal slices with no gap). The 3D MPRAGE was also used to acquire the T_2-weighted image (TR/TE = 3000/402 ms; FoV = 256 × 256 mm^2; voxel size = 1 × 1 × 1 mm^3; 176 sagittal slices with no gap). Then, the field-map was obtained (TR = 800 ms; TE_1 = 10 ms; TE_2 = 13.94 ms; FoV = 240 × 240 mm^2; voxel size = 1.9 × 1.9 × 4.0 mm^3; FA = 25°; 36 sagittal slices with no gap). During the fMRI runs, respiration and pulse oximeter signals were simultaneously recorded using the scanner's built-in wireless pneumatic belt, which was positioned at the level of the abdomen, and a fingertip pulse oximeter placed on the left index finger, respectively.

2.4. Mediation analysis model of the triple network to extract the functional feature of mindfulness

Fig. 2a illustrates the mediation analysis model (MacKinnon, 2008) using the triple networks, in which BOLD signals from the SN are represented by the independent variable $x(t)$ (because of the interoceptive function of the SN, which would be induced by our mindfulness strategy based on focused attention to the physical sensations of breathing). BOLD signals from the DMN are represented by the dependent variable $y(t)$ (because of the self-referential function of the DMN, which would be related to mindfulness status). In addition, BOLD signals from the CEN were assigned as the mediator variable $m(t)$ (because of the goal-oriented cognitive function of the CEN, which would be induced from effort related to the external thermometer bar control). The partial regression coefficient (i.e., slope) value between the SN and the DMN, with the CEN as a mediator (i.e., c' in Fig. 2a), was calculated using Pearson's correlation coefficients between (a) the SN and the DMN (i.e., r_{xy}), (b) the SN and the CEN (i.e., r_{xm}), and (c) the CEN and the DMN (i.e., r_{my}) as follows (see Appendix B for more details):

$$c' = \frac{\left(r_{xy} - r_{xm}r_{my}\right)}{\left(1 - r_{xm}^2\right)} \frac{\sigma_y}{\sigma_x} \quad (1)$$

where σ_x and σ_y were the standard deviations of the signals from the SN and the DMN, respectively. In the triple networks framework, our model of mindfulness based on the mediation analysis was also compared with alternative models using Pearson's correlation analysis between a pair of triple networks and partial correlation analysis across the triple networks (Fig. 2b and c; Appendix A and C for a mathematical comparison).

2.5. Regions-of-interest definition of the triple networks

Regions-of-interest (ROIs) within the triple networks were initialized from a term-based meta-analysis using the Neurosynth repository (neurosynth.org) employing the reverse inference option with a false discovery rate, or FDR $p < 0.01$ (Yarkoni et al., 2011). The keywords used were the "frontoparietal network" for the CEN (since there is no meta-analysis map for the "central executive network"), the "default network" for the DMN, and the "salience network" for the SN. Then, the obtained ROIs in Montreal neurological institute (MNI) space were warped into the individual subject's EPI space (Fig. 3a). This was achieved by applying a "warping matrix", an inverse of the transformation matrix to normalize the subject's first EPI volume to the EPI template in the MNI space used by the statistical parametric mapping software toolbox (SPM8; Lee et al., 2008). These initial ROIs of the triple networks in each subject's EPI space were further fine-tuned for each individual using the estimated triple networks by applying spatial independent component analysis (McKeown et al., 1998b) to the two 3-min resting-state blocks in the two non-rtfMRI runs (as exemplified in Fig. 3b and c; see details in the "***Fine-tuning of regions-of-interest of the triple networks using individual fMRI data***" section of the Supplementary Materials). Fig. 3d shows the group-level fine-tuned ROIs obtained from the one-sample *t*-test across all 60 participants (FDR $p < 0.01$, with a minimum of 10 connected voxels).

2.6. Two real-time fMRI neurofeedback runs and one transfer run: online analysis

2.6.1. Preprocessing

The fMRI volume series from both the two rtfMRI-NF runs and the one transfer run were preprocessed using SPM8. The preprocessing began at 40 s after the cross-fixation period and proceeded in the following order: (a) realignment to the first fMRI volume; (b) de-trending (c) de-spiking (i.e., if the average BOLD intensity across the whole-brain of the current fMRI volume was greater than 110% or lower than 90% of the mean of the average BOLD intensities across previous fMRI volumes, the current fMRI volume was replaced by the fMRI volume of the previous TR) (Garrison et al., 2013); (d) motion censoring (i.e., if the frame-wise displacement, or FD of the current fMRI volume compared with the first fMRI volume was greater than 0.5, the current fMRI volume was replaced by the fMRI volume of the previous TR) (Power et al., 2014); (e) spatial smoothing with an 8 mm full width at half maximum Gaussian kernel; (f) physiological noise correction using the aCompCor method with five principal components (PCs) from the cerebrospinal fluid (CSF) and white matter (WM) regions, respectively (Behzadi et al., 2007). In

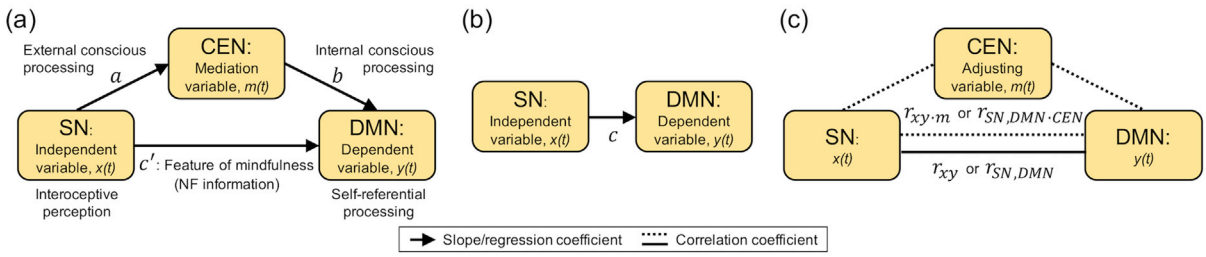

Fig. 2. (a) The proposed mediation analysis model of the triple networks for mindfulness training by rtfMRI-NF and transfer runs (see "Appendix B. ***Regression coefficients (i.e., slopes) from the mediation analysis***" for details). (b) The un-mediated model between the SN and DMN. (c) Simple correlation (r_{xy}, a solid line) and partial correlation ($r_{xy \cdot m}$, dashed lines) models in the triple networks. CEN, central executive network; DMN, default-mode network; NF, neurofeedback; ROI, region-of-interest; SN, salience network.

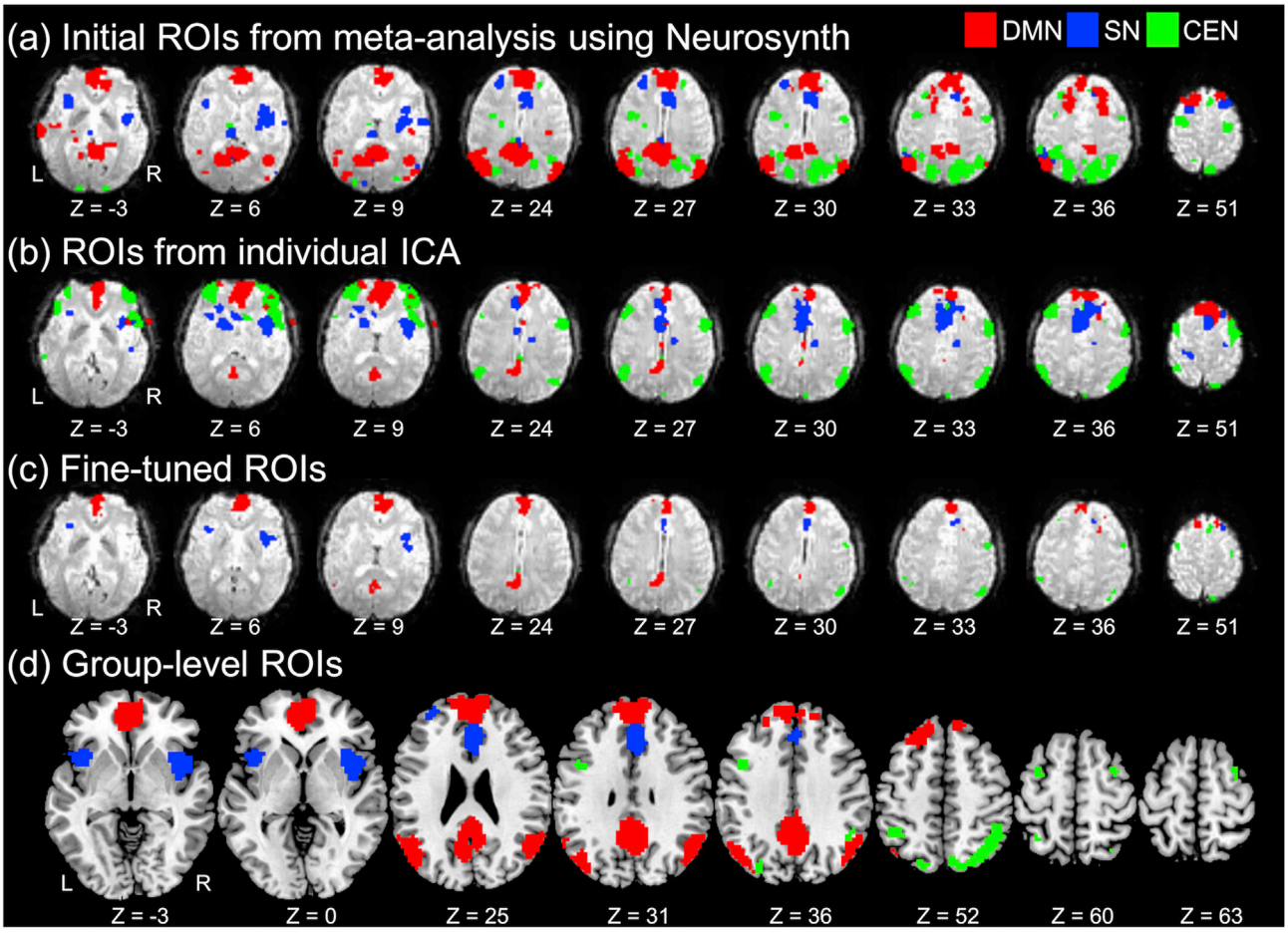

Fig. 3. ROIs of the triple networks. (a) ROIs were initialized from term-based meta-analysis using the Neurosynth repository (neurosynth.org) and projected onto the individual EPI space (false discovery rate or FDR $p < 0.01$). (b) ROIs obtained from the spatial independent component analysis (ICA) using the individual resting-state fMRI data from two non-rtfMRI runs (z-score > 1.96 or uncorrected $p < 0.05$). (c) The fine-tuned ROIs employed in the rtfMRI-runs obtained from the intersection of (a) and (b). (d) Group-level fine-tuned ROIs obtained from the one-sample *t*-test across all participants (FDR < 0.01, with a minimum of 10 connected voxels). See the "***Regions-of-interest definition of the triple networks***" subsection in the Methods section and "***Fine-tuning of regions-of-interest of the triple networks using individual fMRI data***" subsection in the Supplementary Materials for details. L, left; R, right; CEN, central executive network; DMN, default-mode network; rtfMRI, real-time fMRI; SN, salience network.

detail, a priori maps of the WM and CSF regions in MNI space, available in SPM8, were registered into individual native EPI space using the warping matrix. Then, the voxels in the warped a priori maps with a probability greater than 0.7 for the CSF or 0.9 for the WM were used to extract the PCs of the CSF and WM, respectively; (g) nuisance regression applying three translational and three rotational head motion parameters; and (h) bandpass filtering from 0.01 to 0.1 Hz (Kilpatrick et al., 2011; Su et al., 2016) using a fast Fourier transform (Song et al., 2011).

2.6.2. Neurofeedback information

The ROIs of the triple networks were realigned to the first volume in the rtfMRI-NF run, and voxels belonging to the WM and CSF (defined during the aCompCor step) were excluded. Beginning from 90 s (Fig. 1b), the most recent 30 vol (i.e., spanning 43.2 s), including the volume at the current TR, were subjected to mediation analysis to calculate the neurofeedback signal (i.e., $c^{'}$). The neurofeedback signal in the subsequent TR was calculated by advancing by one TR, based on a sliding window approach (Allen et al., 2014). In detail, the average BOLD signals across voxels in each ROI of the triple networks were calculated and then re-scaled to have a mean of 100. Then, the average BOLD signals of the SN (i.e., $x(t)$) and the CEN (i.e., $m(t)$) were normalized between 0 and 1 by subtracting the minimum value of the BOLD signal followed by dividing by the difference between the maximum and minimum of the BOLD signal (i.e., $\frac{x(t)-\min(x(t))}{\max(x(t))-\min(x(t))}$ and $\frac{m(t)-\min(m(t))}{\max(m(t))-\min(m(t))}$, where $\min(\cdot)$ and $\max(\cdot)$ are the functions calculating the minimum and maximum values, respectively). These normalized signals, along with a vector of ones to estimate the bias term b_1, were used as regressors in the general linear model framework (see "Appendix B" for details). Since $y(t)$ was re-scaled to have a mean of 100, the re-scaled $y(t)$ represents the percentage signal change compared to the mean. For instance, if the mean of $y(t)$ (i.e., baseline BOLD intensity of $y(t)$) was originally 1000 and $y(t_i) = 1010$ at time point t_i, then the percentage signal change of $y(t_i) = (1010–1000)/1000 \times 100 = 1\%$. Now, when we scaled $y(t)$ to have a mean of 100 by dividing $y(t)$ by 10, then $y(t_i) = 101$. The bias term, b_1 would estimate a mean of 100 of the re-scaled $y(t)$, and thus, $y(t) - b_1 = c^{'}x(t) + bm(t) + e_1(t)$, where the left side of the equation (i.e., $y(t) - b_1$) becomes the percentage (%) signal change in $y(t)$. Thus, the regression coefficients $c^{'}$ as well as b denote the percentage signal changes for each of the $x(t)$ and $m(t)$ regressors (which were normalized between 0 and 1). $c^{'}$ was used for the neurofeedback interface, presented as a thermometer bar. To set the maximum and minimum range of the bar, a pilot study was conducted with three subjects (data not shown), and the highest and lowest levels of the thermometer bar were set to $c^{'}$ values of +0.5 and −0.5, respectively.

2.6.3. Software toolbox

Our in-house software toolbox (implemented in a MATLAB environment; version R2016b), which has been used in our previous rtfMRI-NF studies (Kim et al., 2015a; Lee et al., 2008, 2009, 2012c; Yoo et al., 2007, 2008), was updated for the present study. The rtfMRI-NF toolbox was executed on a desktop computer (Intel Core i7-3770 CPU @ 3.40 GHz, 16-GB RAM, 256-GB SSD hard drive, Windows 7) connected to an MRI console computer via TCP/IP using the "net use" command. Thereby, the raw fMRI volumes that were reconstructed in the MRI console computer became available in the desktop computer. Then, the fMRI volumes of the two rtfMRI-NF runs on the desktop computer were used to generate neurofeedback information obtained from the mediation analysis. The time delay from the acquisition of a raw fMRI volume to the presentation of neurofeedback information (i.e., c') was less than a TR.

2.7. Offline analysis

The main purpose of the ambulatory training was to provide an opportunity for meditation-naïve participants to become familiar with the task strategies (Table 1). However, potential group difference may be caused by the smartphone-based ambulatory training, such as in overall behavioral scores and in their improvements over time. Thus, this possibility and a potential interaction with the rtfMRI-NF training were investigated (please refer to the section "***Analysis of the behavioral data obtained from the smartphone-based ambulatory training***" in the Supplementary Materials for details).

The participants' rating scores collected during the MRI session were used to evaluate the two rtfMRI-NF runs and one transfer run. Compared with the online analysis by applying the aCompCor method, potential physiological artifacts present in the BOLD signals could be further reduced by applying the RETROICOR method using pulse oximeter and respiration belt signals (Glover et al., 2000). In detail, the two phasic signals extracted from the respiration belt and pulse oximeter signals were down-sampled to have the same temporal resolution as the BOLD signals (i.e., TR) using the Physiological Log Extraction for Modeling (PhLEM) Toolbox (Verstynen and Deshpande, 2011). Then, the least-squares algorithm was used to regress these physiological data out of the BOLD signals (Behzadi et al., 2007; Chai et al., 2012; Kim et al., 2013, 2015a, 2015b; Lee et al., 2012b; Song et al., 2011).

A two-sample *t*-test was used to compare cardiac and respiratory cycles between the experimental and control groups. Because of head motion (i.e., FD > 0.5 for longer than half of the mindfulness period in any of the rtfMRI-NF runs or the transfer run), eight participants were excluded from further analysis (two subjects in the experimental group and their matched subjects in the control group; two subjects in the control group and their matched subjects in the experimental group). Table S2 summarizes their sociodemographic information and psychological traits as well as head motions. Thus, 52 participants (26 participants per group) were included in the analysis of this study.

Next, the regression coefficient levels in the mediation analysis model of the triple networks (i.e., a, b, and c') calculated from the offline and online analyses were compared. A correlation analysis was applied to the average of the two mindfulness scores (i.e., SMS_S) and the task-performance feedback score to evaluate the possibility of whether our neurofeedback information (i.e., c') reflected the level of mindfulness. To remove any potential residual effects from a rehearsal during the instruction period of the mindfulness strategy (i.e., 75 s–85 s) before the mindfulness task-period began, for this correlation analysis, the average c' value across all the 43.2 s windows was calculated by excluding the 43.2 s (i.e., 30 volumes) at the beginning of the 300 s task-period. As such, alternative regression coefficient levels (i.e., a or b) may represent the level of mindfulness, and this possibility was also investigated using average mindfulness scores and task-performance feedback scores in the correlation analysis with their corresponding regression coefficient levels. Additionally a bootstrapping method has been used to conduct a statistical analysis of the difference in correlations (e.g., "c' vs. mindfulness scores" – "b vs. mindfulness scores", or $CC(c', SMS_S) - CC(b, SMS_S)$ to remove potential bias from the mediation effect b from the CEN to the DMN) (Terhune et al., 2014) (Table 3). Also investigated was (a) a potential association between the amount of mediation (i.e., ab) and the mindfulness/task-performance scores and (b) whether the amount of mediation was equivalent between the two groups when the direct effect (i.e., c') was compared between them. The potential association between the total effect (i.e., c; Fig. 2b) and mindfulness/task-performance scores has also been investigated. Moreover, the possibility that the FC levels calculated from Pearson's correlation analysis or partial correlation analysis represented the level of mindfulness was also investigated. Potential outliers in the behavioral data as well as the regression coefficients (i.e., slopes) from the mediation analysis and simple/partial correlation coefficients were identified (see "***Definition of outliers based on median absolute deviation (MAD)***" for details in the Supplementary Materials) and subsequently removed from the correlation analysis between the behavioral data and the brain data.

2.8. Control analyses

2.8.1. Correlation analysis between paired participants for each of the reported mindfulness/task-performance scores and c' values

In the rtfMRI-NF training, participants were asked to increase the thermometer bar (i.e., c') while deploying the mindfulness strategy based on attention to the physical sensation of breathing. Subsequently, correlations between the c' values and the mindfulness/task-performance scores were investigated to evaluate the efficacy of the rtfMRI-NF training. The possibility that this "dual-task" setting might have resulted in the significant positive association between c' and the mindfulness/task-performance scores needs to be addressed. To evaluate this, we conducted control analyses to determine any (a) correlation between paired participants (who watched the same thermometer bar) for each of the reported mindfulness/task-performance scores and c' values; (b) association between the mindfulness scores and potentially alternative mindfulness-related features of the brain such as activations in the triple networks; (c) association between cardiac/respiratory measurements and brain data or mindfulness/task-performance scores. To evaluate possibility (a), correlation analyses of the c', SMS_S, and TPF scores across the paired participants were conducted using the data obtained from the rtfMRI-NF runs and the transfer run. Evaluations of the possibilities of (b) and (c) are described in the following sub-sections.

2.8.2. Percentage blood-oxygenation-level-dependent (BOLD) signal changes vs. mindfulness

It may be possible that activations in one or more of the ROIs in the triple networks may have changed in the rtfMRI-NF setting and become associated with mindfulness. To evaluate this possibility, a correlation analysis was conducted between the activation levels in the ROIs and the mindfulness/task-performance scores. The candidate ROIs of the sub-regions of the triple networks were defined from the group-level ROIs of the triple networks (Fig. 3d). In detail, the SN was sub-divided into the dorsal anterior cingulate cortex of the SN (SN_{dACC}) and the bilateral anterior insular cortices of the SN (SN_{INS}) (Seeley et al., 2007) (Fig. S8). The DMN was sub-divided into the anterior part of the DMN (aDMN), which includes the medial prefrontal cortex, or mPFC, and the posterior part of the DMN (pDMN), which includes the PCC ($pDMN_{PCC}$) and the bilateral inferior parietal lobule of the pDMN ($pDMN_{IPL}$) (Kim and Lee, 2011) (Fig. 10). The CEN was sub-divided into the frontal part of the CEN (i.e., the bilateral frontal area of the CEN (CEN_F)) and bilateral parietal area of the CEN (CEN_P) (Menon, 2011) (Fig. S8). These sub-regions of each of the triple networks were defined using the Xjview software toolbox (www.alivelearn.net/xjview). In addition, specific seed regions of the DMN such as the mPFC (MNI coordinate: [−6, 52, −2] mm) and PCC ([−8, −56, 26] mm) consisting of spheres 9 mm in radius have also

been employed as ROIs (Brewer et al., 2011; Garrison et al., 2013).

The raw fMRI volumes were preprocessed according to the following sequence: realignment to the first EPI volume, detrending, spatial smoothing with an 8 mm full width at half maximum Gaussian kernel, physiological noise correction using each of the 5 PCs from the CSF and WM, nuisance regression using six motion parameters, and band-pass filtering between 0.01 and 0.1 Hz. The percentage BOLD (pBOLD) signals during the task-period (i.e., 97.2 s–390 s after the exclusion of 5 volumes from task onset to remove any confounding effect from the rehearsal phase spanning 75 s–85 s) were calculated from the preprocessed data using a baseline BOLD intensity defined as the average BOLD intensity between 10 and 40 s during the first cross-fixation period (Fig. 1b). Then, average pBOLD intensity was calculated across the task-period after excluding the pBOLD intensity outliers (see the Supplementary Material section, "***Definition of outliers based on median absolute deviation (MAD)***" for details) and excluding the EPI volumes featuring severe head motion (FD score > 0.5).

2.8.3. Cardiac/respiratory cycles vs. regression coefficients in the mediation analysis and/or mindfulness/task-performance scores

The possibility of whether the cardiac/respiratory cycles during the training may have contributed to the changes in (a) the regression coefficients from the mediation analysis and/or (b) the mindfulness scores and task-performance feedback scores was investigated. The cardiac (beats/minute) and respiratory (breaths/minute) cycles were extracted using the PhLEM toolbox.

2.9. Effective connectivity of the triple networks

Our hypothesized model suggested that interoceptive perception in the SN may induce mindfulness states in the DMN, mediated by the CEN. However, it is still unclear whether the interoceptive perception caused the mindfulness status or whether, conversely, the mindfulness status itself caused the enhancement in interoceptive perception. Another possibility is that the triple networks may have been causally linked to each other and that this causal connection may have been characterized differently based on both the type of training run (i.e., rtfMRI-NF run vs. transfer run) and the type of the NF information provided (i.e., contingent for the experimental group vs. non-contingent for the control group). To investigate this possibility, spectral dynamic causal modeling (spDCM) in SPM12 (www.fil.ion.ucl.ac.uk/spm/software/spm12) that has been gainfully applied to the resting-state fMRI data was used (Friston et al., 2014). The detailed analysis step can be found in the Supplementary Materials ("***Effective connectivity among the triple networks using spectral dynamic causal modeling (spDCM)***").

3. Results

3.1. Data from subjective ratings and raw fMRI

The completion ratio of the smartphone-based ambulatory training sessions (i.e., 86.67% ± 16.47 for the experimental group vs. 87.00% ± 12.64 for the control group) did not statistically differ between the two groups ($p = 0.93$; Table S1). The results from the ambulatory training suggested that there was no main effect of group, sequence-of-condition for mindfulness and mind-wandering strategies, or their interaction with the rtfMRI-NF training in (a) the PSS, MDMQ, SMS, VAS, and TPF scores obtained on the last day of the ambulatory training (Fig. S1d) and (b) the MDMQ, SMS, and VAS scores obtained in the pre-MRI session (Fig. S2) (see "***Data from smartphone-based ambulatory training***" for details in the Supplementary Materials).

Fig. 4a shows that, based on the MDMQ results, mood changed differently between the two groups in the MRI session. They both showed significantly higher levels of mindfulness (measured by the SMS; $p < 10^{-3}$, obtained from a paired *t*-test with the *p*-value corrected from 10,000 random permutations) after the MRI session than before. There were no significant changes in participant stress levels. Fig. 4b shows that there were no significant differences in the mindfulness or task-performance scores across runs or across groups. In addition, Fig. 4c shows that the regression coefficient levels obtained from the online and offline analyses did not differ.

The cardiac cycle (i.e., mean ± STD; 62.6 ± 8.6 beats per minute for the experimental group and 64.5 ± 9.8 for the control group, $p = 0.26$ from the two-sample *t*-test) and respiratory cycle (11.6 ± 3.9 breaths per minute for the experimental group and 11.5 ± 4.8 for the control group, $p = 0.87$) did not statistically differ between the two groups. The average (±STD) FD values of head motion from the resting-state blocks for each of the two non-rtfMRI runs were 0.11 (±0.05) for the first run and 0.12 (±0.08) for the second run. There was no volume for which the FD value was above 0.5, and the FD values across the rtfMRI-NF runs and the transfer run did not significantly differ between the two groups (i.e., 0.13 ± 0.08 for the experimental group and 0.12 ± 0.07 for the control group; $p = 0.88$ from the two-sample *t*-test).

3.2. Regression coefficient feature of mindfulness in the mediation analysis framework

Fig. 5a shows the line plots of the average c' level, with standard errors in the shaded areas. Overall, the regression coefficient (i.e., slope) levels of the experimental group were significantly greater than those of the control group at several time-points (i.e., those marked by an asterisk *; paired difference was also plotted in gray). Average slope levels (i.e., c' levels across the 300 s of each run did not statistically differ between the two groups, although the mean slope level of the experimental group was higher than that of the control group ($p = 0.32$, 0.14, and 0.58 for the rtfMRI-NF run#01, #02, and transfer run, respectively). Fig. 5b shows that the neurofeedback signal (i.e., c') was significantly correlated with the mindfulness and task-performance feedback scores in the rtfMRI-NF runs, only in the experimental group. Fig. S3 shows that those positive correlations from the rtfMRI-NF runs were retained even after the subtraction of the respective correlations between the mediation effect (i.e., *b*) and the mindfulness scores and task-performance feedback scores. The corresponding 95% CIs were [0.05, 0.88] for the correlation with mindfulness scores and [0.10, 0.92] for the correlation with the task-performance feedback scores.

3.3. Regression coefficient levels from other pairs of the triple networks in the mediation analysis framework

Fig. 6a shows that there was a significant positive correlation between the regression coefficient (i.e., slope) from the SN to the CEN (i.e., *a*) and the task-performance feedback scores for the control group. Fig. 6b shows that the slope levels from the CEN to the DMN (i.e., *b*) of the control group in the rtfMRI-NF runs presented weakly suggestive and significantly positive correlations with the mindfulness and task-performance feedback scores, respectively. On the other hand, the slope (i.e., *b*) and the task-performance feedback scores of the experimental group showed a weakly suggestive negative correlation in the rtfMRI-NF runs. Fig. 7a shows that the mediation effect *ab* values presented significant positive correlations with the mindfulness scores and task-performance feedback scores in the rtfMRI-NF runs only for the control group. In the time plots, the mediation effect, *ab* values did not significantly differ between two groups, particularly when the direct effect, c' values, significantly differed between two groups (small square boxes). Fig. 7b shows that the slope, *c* (i.e., the total effect from the SN to the DMN) presented significant correlation and suggestive positive correlation with the mindfulness scores and task-performance feedback scores, respectively, in the rtfMRI-NF runs of the experimental group. However, the time plots show that the time points that featured significantly greater intensities from the experimental group than the control group were more associated with the direct effect (i.e., c'; rectangular

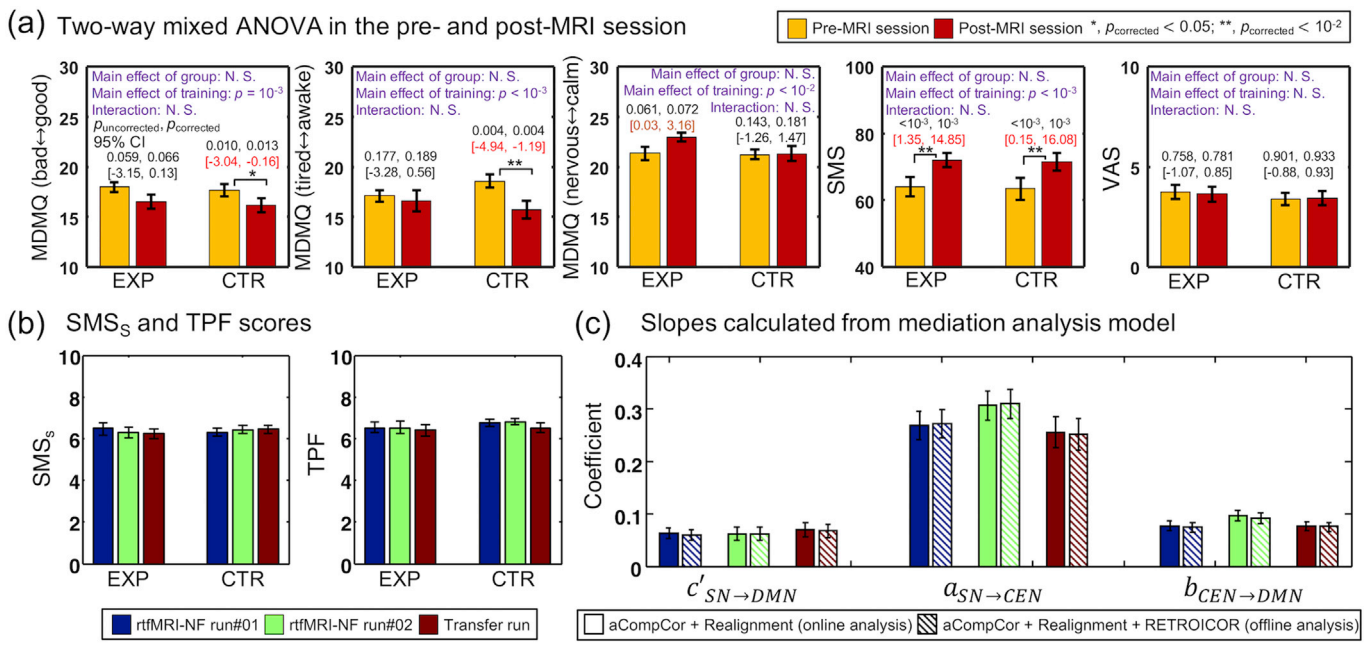

Fig. 4. Behavioral data (a–b) and regression coefficient (i.e., slope) levels from the online and offline analyses (c). (a) Behavioral data obtained from Multidimensional Mood State Questionnaire (MDMQ), State Mindfulness Scale (SMS), and Visual Analog scale for Stress perception (VAS), scores obtained before (pre-MRI) and after (post-MRI) the MRI session. A two-way (i.e., 2 [groups; EXP or CTR] × 2 [training types; pre- or post-MRI session]) mixed analysis-of-variance was applied. The confidence intervals (CIs) in red and orange are identified as "significant" and "weakly suggestive", respectively. (b) Scores from the short version of the SMS (or SMS$_S$) and task-performance feedback (TPF) obtained in the two rtfMRI-NF runs and one transfer run. (c) Slope levels calculated from the mediation analysis model using the triple networks in the online analysis (i.e., nuisance regression with three translational and three rotational head motion parameters, and physiological noise correction using aCompCor) and the offline analysis (i.e., the same nuisance regression and physiological noise correction using aCompCor and, additionally, RETROICOR). See the "***Overall study protocol***" subsection in the Methods section and "***Data from subjective ratings and raw fMRI***" subsection in the Results section for details. The vertical bars and whiskers represent the mean and standard error, respectively. The *a*, *b*, and *c*' are the slope levels between the corresponding pairs in the triple networks (Fig. 2). aCompCor, a component based noise correction method; CEN, central executive network; CTR, control group; DMN, default-mode network; EXP, experimental group; rtfMRI-NF, real-time fMRI neurofeedback; RETROICOR, RETROspective Image CORrection; SN, salience network.

box) than the total effect (i.e., *c*; asterisk). Also, the statistical significance was stronger when considering *c*' (i.e., $p = 0.007$ with the mindfulness scores and $p = 0.001$ with the task-performance scores; Fig. 5b) than when considering *c* (i.e., $p = 0.04$ and $p = 0.01$; Fig. 7b).

3.4. FC levels from Pearson's correlation and partial correlation analyses

Fig. 8a shows that the FC levels (from simple correlation coefficients) between the SN and the DMN resulted in suggestive positive correlations with the mindfulness scores in both the rtfMRI-NF and transfer runs, but only from the experimental group. In the time plots, the time-points that showed greater FC levels for the experimental group than the control group became scarce in the second rtfMRI-NF run (cf., Fig. 5a).

Fig. 8b shows that the FC levels (from partial correlation coefficients) between the SN and the DMN, with the adjusting variable from the CEN, presented significant and suggestive positive correlation with the mindfulness scores in both the rtfMRI-NF runs and the transfer run only with the experimental group. The corresponding statistical significance of the correlation coefficient in the rtfMRI-NF run ($p = 0.002$) was slightly greater than that of the mediation analysis ($p = 0.007$; Fig. 5b). However, the time-points that showed statistically greater ($p < 0.05$) FC levels (i.e., $r_{SN,DMN \cdot CEN}$) from the experimental group than the control group were fewer compared to the time plots of *c*' (cf., Fig. 5a).

3.5. Results of the control analyses

Fig. 9 shows that there was no meaningful correlation of the *c*' values, mindfulness scores, or task-performance feedback scores between the paired participants across the two groups during both the rtfMRI-NF and transfer runs. Fig. 10 shows that there were significant correlations between the pBOLD intensities of the sub-regions of the DMN and mindfulness/task-performance scores. Particularly, it is notable that the significant negative correlations between the aDMN/mPFC activations and the mindfulness scores in the rtfMRI-NF runs are only from the experimental group. Also, the negative correlations between the PCC activations and the mindfulness scores, which were potentially weakly suggestive in the rtfMRI-NF runs, became significant in the transfer run only with the experimental group. The average activations during the task-period in the PCC area for the experimental group (mean ± STD; −0.012 ± 0.067 in the rtfMRI-NF run#01 and −0.014 ± 0.073 in the rtfMRI-NF run#02) were slightly lower compared to those for the control group (−0.009 ± 0.060 and 0.003 ± 0.006) during the rtfMRI-NF runs. On the other hand, the activation levels in the PCC for the control group (−0.010 ± 0.086) were slightly lower than those from the experimental group (−0.005 ± 0.081) during the transfer run. However, these differences were not statistically significant between the two groups. Fig. S8 shows that there were weakly suggestive and potentially weakly suggestive correlations between the activations in the sub-regions of the SN and CEN and mindfulness/task-performance scores, but there was no significant correlation. Fig. S9 shows example time plots of the PCC activations of a pair of participants who reported high average mindfulness scores across the two rtfMRI-NF runs and one transfer run (8.3 ± 0.3 from the participant in the experimental group, 7.7 ± 0.6 from the participant in the control group). Fig. 11 shows that the cardiac cycles showed a suggestive negative correlation with slope *a*, a significant negative correlation with slope *b*, and a weakly suggestive positive correlation with the mindfulness scores, but only from the experimental group during the rtfMRI-NF runs. There was no meaningful correlation under other conditions such as when using the respiratory cycles or with the control group.

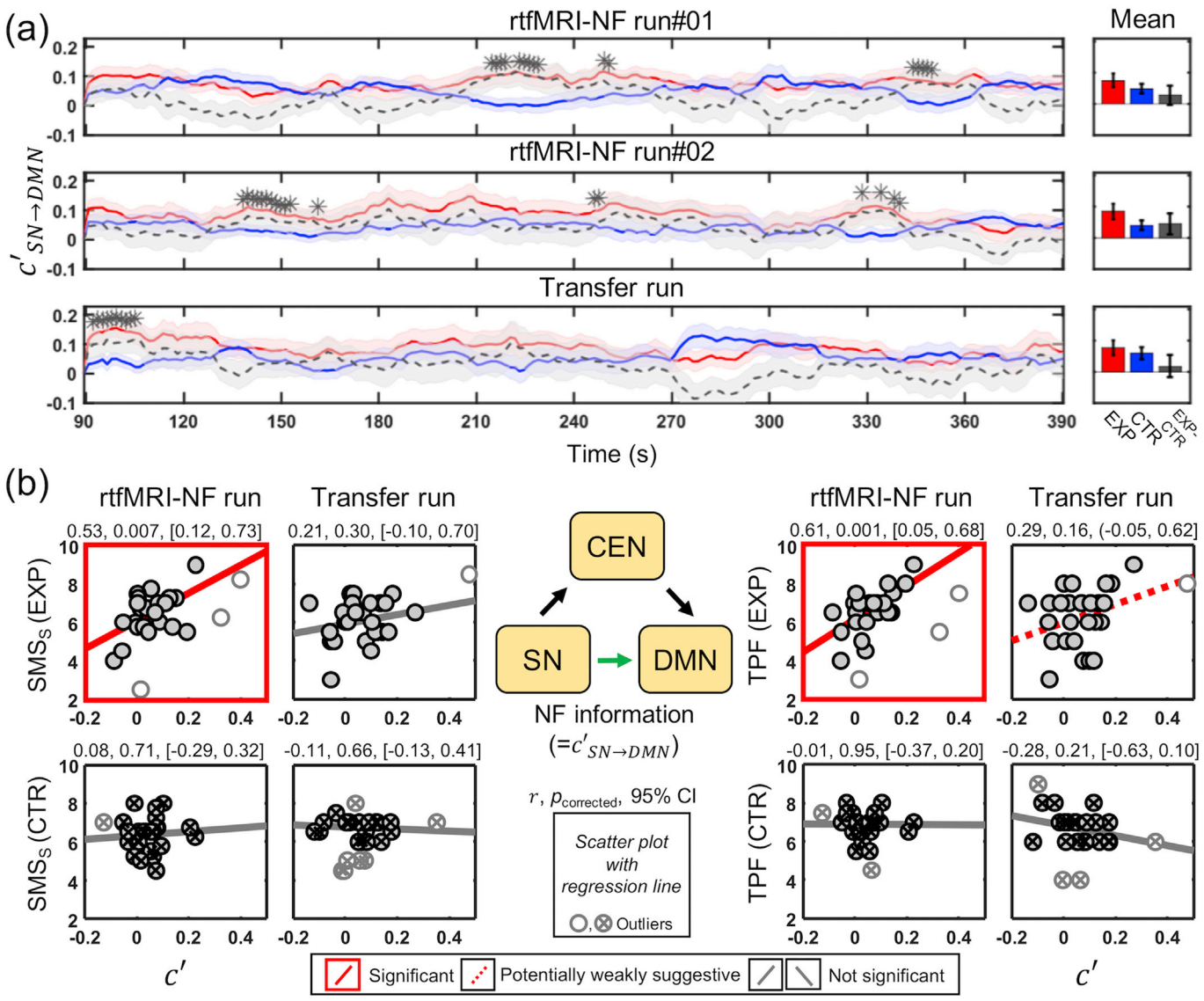

Fig. 5. The partial regression coefficient (i.e., slope) levels from the SN to the DMN mediated by the CEN (i.e., *c*') and their association with the SMS$_S$ (i.e., mindfulness scores) and TPF scores. (a) Time plots of the *c*' value along the two rtfMRI-NF runs and one transfer run (line: mean across all subjects; shaded areas: standard errors of the mean). Any time-point where the paired differences (dark gray) of slope values between the experimental (red) and control (blue) groups were significantly non-zero (corrected $p < 0.05$ excluding outliers) was denoted by an asterisk *. (b) Scatter plots using the neurofeedback information (i.e., *c*') in the mediation analysis and SMS$_S$ or TPF scores for each of the two groups (top row: experimental group; bottom row: control group). CEN, central executive network; CTR, control group; DMN, default-mode network; EXP, experimental group; rtfMRI-NF, real-time fMRI neurofeedback; SMS$_S$, short version of the State Mindfulness Score; SN, salience network; TPF, task-performance feedback. Detailed information about outliers, *p*-value correction of correlation coefficient (i.e., *r*), confidence interval (CI), and stratified scenarios of statistical significance is presented in Table 3.

3.6. *Effective connectivity of the triple networks*

The fully-connected model with bi-directional effective connectivity between the pairs within the triple networks was selected as an optimal model for both the rtfMRI-NF and the transfer runs. Fig. 12(a and b) show that the experimental group presented significant positive effective connectivity (i) from the CEN and DMN to the SN in the rtfMRI-runs and (ii) from the SN and CEN to the DMN in the transfer run. The self-connection within the DMN showed significant negative correlation with the mindfulness scores only during the rtfMRI-NF runs. Fig. 12(c and d) show that the control group presented significant positive effective connectivity (i) from the CEN to the SN in the rtfMRI-NF runs and (ii) from the CEN to the DMN in the transfer run. The mindfulness scores showed weakly suggestive correlation or suggestive negative correlation with the self-connections within the SN in the rtfMRI-NF runs and within the CEN in the transfer run, respectively, for the control group. The task-performance scores showed weakly suggestive positive correlation with the inter-network connection from the CEN to the DMN in the transfer run for the control group.

4. Discussion

4.1. *Summary*

In this study, we demonstrated that the partial regression coefficient level (i.e., direct effect, *c*') from the SN to the DMN, mediated by the CEN in the mediation analysis framework, appears to be one of the potential features of mindfulness in the rtfMRI-NF setting. The validity of this regression coefficient (i.e., slope) feature was further evaluated from its statistically significant positive association with the mindfulness and

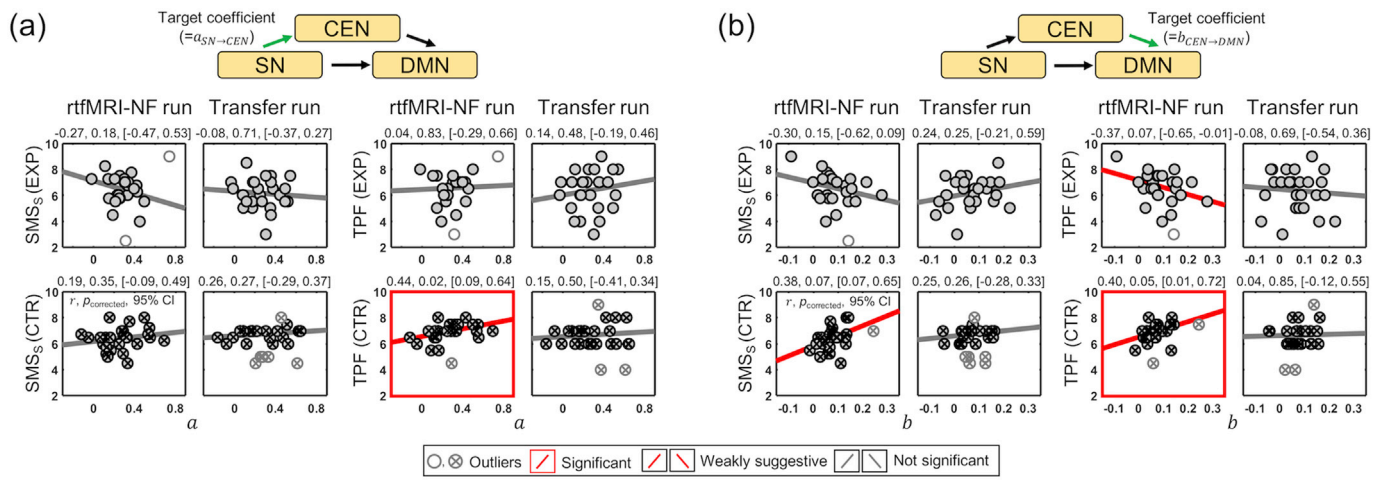

Fig. 6. Scatter plots of (a) the regression coefficient (i.e., slope) levels from the SN to the CEN (i.e., *a*) and the SMS$_S$/TPF scores and (b) the slope levels from the CEN to the DMN (i.e., *b*) and the SMS$_S$/TPF scores. CEN, central executive network; CTR, control group; DMN, default-mode network; EXP, experimental group; rtfMRI-NF, real-time fMRI neurofeedback; SMS$_S$, short version of the State Mindfulness Scale; SN, salience network; TPF, task-performance feedback. Detailed information about outliers, *p*-value correction of correlation coefficient (i.e., *r*), confidence interval (CI), and stratified scenarios of statistical significance is presented in Table 3.

task-performance scores independently measured after each rtfMRI-NF run and transfer run. These positive correlations between c' and the mindfulness scores (i.e., CC(c', SMS$_S$)) and between c' and the task-performance feedback scores (i.e., CC(c', TPF)) remained significant even after the correlation coefficients between *b* and SMS$_S$ (i.e., CC(*b*, SMS$_S$)) and TPF (i.e., CC(*b*, TPF)) were subtracted. The regression coefficient (i.e., total effect, *c*) from the SN to the DMN also showed significant correlation with the mindfulness scores and task-performance feedback scores in our rtfMRI-NF runs. It is notable, however, that the level of statistical significance when considering the direct effect from the SN to the DMN (c'; by excluding the indirect/mediation effect via the CEN) was stronger than that when considering the total effect from the SN to the DMN (*c*; Fig. 7b). This suggests that the efficacy of our rtfMRI-NF training of mindfulness was better explained in terms of c' which excludes the mediating effect via the CEN (i.e., *ab*) from the total effect from the SN to the DMN (i.e., *c*) and this supports our hypothesis that c' is a potential mindfulness feature in our rtfMRI-NF setting. In addition, the participants were able to enhance this functional feature of mindfulness when the partial regression coefficient feature was used as contingent neurofeedback information. Furthermore, the regression coefficient levels from the other pairings of the triple networks did not appear to reflect the mindfulness level. In addition, enhancement of the FC level was not evident during the rtfMRI-NF runs when the FC levels were calculated either from Pearson's correlation analysis (between the SN and the DMN) or partial correlation analysis (between the SN and the DMN, as adjusted by the CEN).

4.2. Changes in the subjective ratings of mindfulness and task-performance scores in the MRI session

Interestingly, it appeared that participant mood was changed after the MRI session (i.e., significant decreases in good–bad and awake–tired moods for the control group and a weakly suggestive increase in the calm–nervous mood for the experimental group; Fig. 4a). This may be because of the effect of having the two rtfMRI-NF runs with contingent or non-contingent NF information, which was the only difference between the two groups. There was no significant group-based difference between the mindfulness or task-performance scores obtained from the rtfMRI-NF runs and the transfer run. However, the mindfulness and task-performance scores were significantly correlated with the regression coefficient levels from the SN to the DMN, as mediated by the CEN, but for the experimental group only. During the debriefing session, approximately half of the participants gave a verbal or written assessment of their performance during the rtfMRI-NF runs. Twelve of these subjects from the experimental group reported that they noticed that the thermometer bar had changed as they expected, and three subjects in the group reported that it had not changed as they expected. On the other hand, in the control group ten subjects reported that the thermometer bar did not change as they had expected, although they reported that they had managed to increase the bar by enhancing their mindfulness level, and two subjects reported that the thermometer bar had changed as they expected.

4.3. Potential confounding physiological artifacts due to mindfulness strategy

In our study, focused attention on the physical sensations of breathing was adopted as a mindfulness strategy, which may confound the BOLD signal (Birn et al., 2008; Raj et al., 2001). Thus, we made a significant effort to reduce potential respiration artifacts in the BOLD signal by using aCompCor-based physiological noise removal in the online analysis and additionally RETROICOR in the offline analysis (Behzadi et al., 2007; Glover et al., 2000). The resulting regression coefficient (i.e., slope) levels obtained from the online analysis were comparable to those obtained from the offline analysis (Fig. 4c). This indicates that the physiological artifacts in the BOLD signal were still sufficiently reduced when slope levels were calculated during the online analysis. In Fig. 4c, the fact that the slope levels between the SN and the CEN (i.e., *a*) were greater than those between the SN and the DMN (i.e., c') and those between the CEN and the DMN (i.e., *b*) is in accordance with previous studies (Farb et al., 2007; Mooneyham et al., 2016). For example, in mindfulness the CEN integrates the moment-to-moment input from a variety of somatic and sensory systems received in the SN by conscious executive processing (Mooneyham et al., 2016).

4.4. Correlation between alternative regression coefficient levels across the triple networks and subjective ratings

In our mediation analysis framework, the regression coefficient (i.e., slope) levels between the CEN and the DMN showed weakly suggestive and significant positive correlations with mindfulness and task-performance feedback scores, respectively, for the control group in the rtfMRI-NF runs (Fig. 6b). Also, the mediation effect *ab* consistently showed significant positive correlation with the mindfulness/task-performance scores in only the rtfMRI-NF runs of the control group

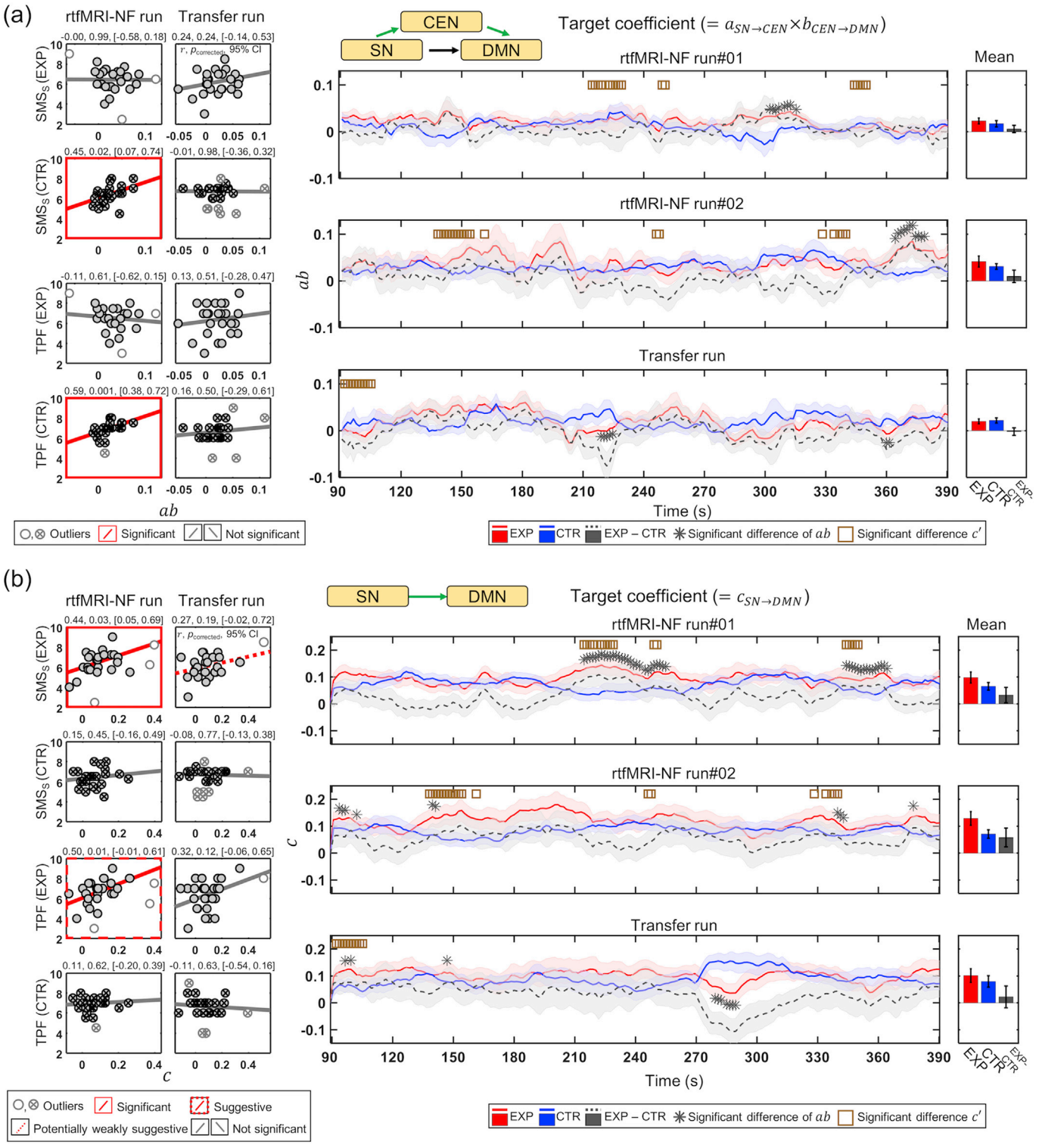

Fig. 7. Scatter plots of (a) the regression coefficient (i.e., slope) values of *ab* and SMS_S/TPF scores and (b) the slope value of *c* and the SMS_S/TPF scores and their time plots (line: mean across all subjects; shaded areas: standard errors of the mean) across the two rtfMRI-NF runs and one transfer run along with the mean and standard error across the time points. CTR, control group; DMN, default-mode network; EXP, experimental group; rtfMRI-NF, real-time fMRI neurofeedback; SMS_S, short version of the State Mindfulness Scale; SN, salience network; TPF, task-performance feedback. Detailed information about outliers, *p*-value correction of correlation coefficient (i.e., *r*), confidence interval (CI), and stratified scenarios of statistical significance is presented in Table 3.

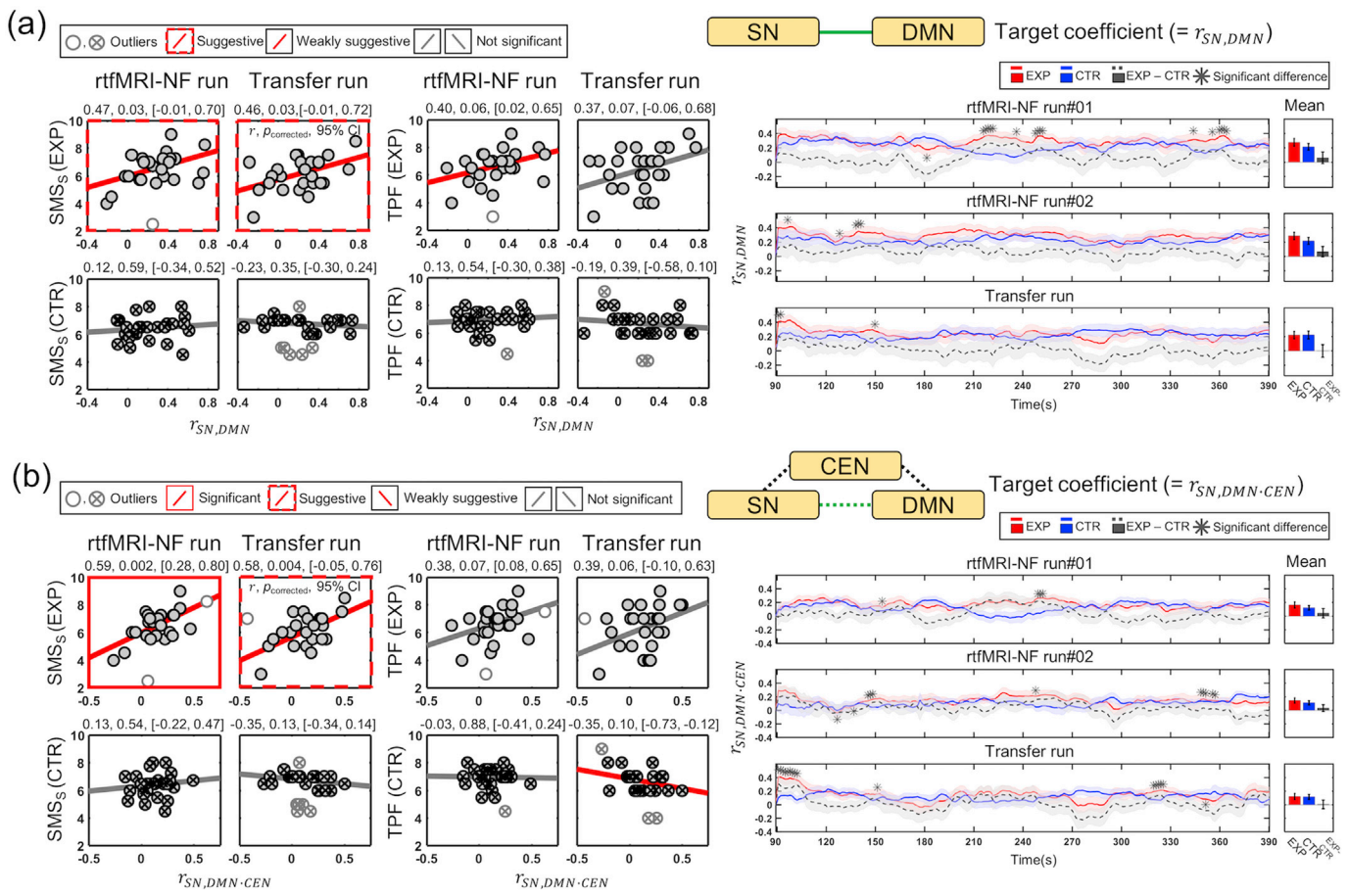

Fig. 8. Scatter plots using the functional connectivity (FC) levels between either (a) the SN and DMN from the Pearson's correlation analysis or (b) the SN and DMN with the adjusting variable from the CEN from the partial correlation analysis, and either the SMS_S or TPF scores. The line plots of the FC levels for each of the two rtfMRI-NF runs and one transfer run (line: mean across all subjects; shaded areas: standard errors of the mean). CEN, central executive network; DMN, default-mode network; SN, salience network; SMS_S, short version of the State Mindfulness Score; TPF, task-performance feedback; rtfMRI-NF, real-time fMRI neurofeedback; EXP, experimental group; CTR, control group. Detailed information about outliers, *p*-value correction of correlation coefficient (i.e., *r*), confidence interval (CI), and stratified scenarios of statistical significance is presented in Table 3.

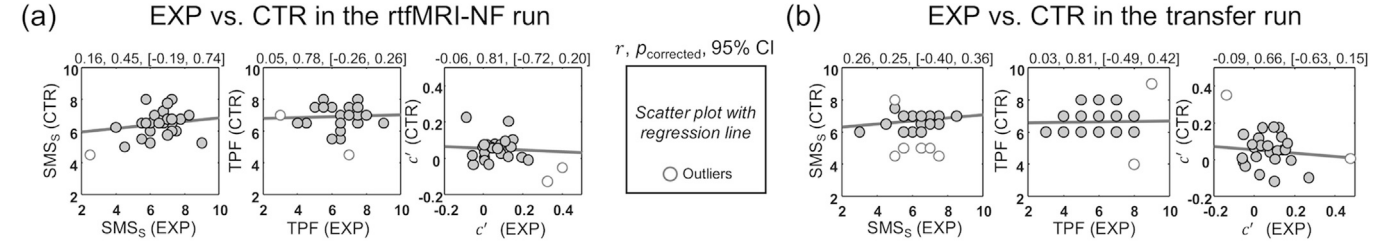

Fig. 9. Scatter plots of the *c*' values, SMS_S scores and TPF scores from the paired participants across the two groups in (a) the rtfMRI-NF run and (b) transfer run. CTR, control group; EXP, experimental group; rtfMRI-NF, real-time fMRI neurofeedback; SMS_S, short version of the State Mindfulness Scale. TPF, task-performance feedback. Detailed information about outliers, *p*-value correction of correlation coefficient (i.e., *r*), and confidence interval (CI) is presented in Table 3.

(Fig. 7a). Moreover, it is notable that this significant positive correlation using the overall mediation effect *ab* was stronger than the positive correlation obtained when using either *a* or *b* alone (cf., Figs. 7a and 6). This finding indicates that the participants in the control group reported mindfulness and task-performance scores based on how much they "controlled" the thermometer bar. This is likely because the CEN, which has been associated with goal-oriented cognition (Beaty et al., 2015; Christoff et al., 2016; Mooneyham et al., 2016; Sridharan et al., 2008; Uddin, 2015), elevated neuronal activation when the participants tried to control the level of the bar. In turn, this may have induced a greater mindfulness status, which was reflected in the self-referential processing of the DMN (Hasenkamp and Barsalou, 2012; Mooneyham et al., 2016; Wells et al., 2013). On the other hand, the task-performance scores of the participants in the experimental group were inversely correlated with the slope levels between the CEN and the DMN in the rtfMRI-NF runs (Fig. 6b). This indicates that the participants in the experimental group rated low task-performance scores when they tried to control the level of the bar.

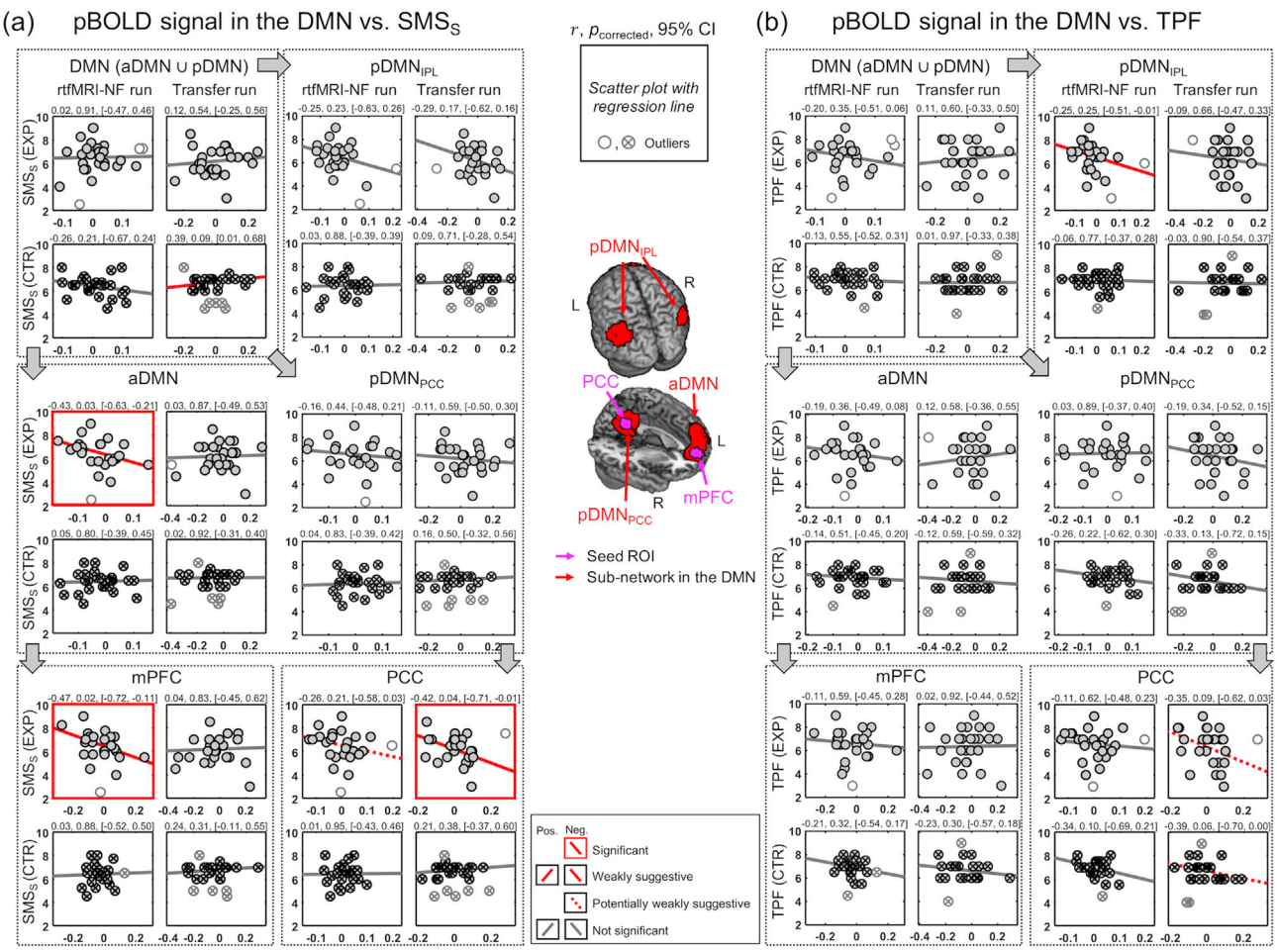

Fig. 10. Scatter plots of the percentage blood-oxygenation-level-dependent (pBOLD) signal obtained from each ROI within the default-mode network (DMN) and the SMS_S (a) or TPF (b) scores in the rtfMRI-NF runs and transfer run. L, left; R, right; aDMN, anterior DMN; CTR, control group; EXP, experimental group; IPL, inferior parietal lobule; Neg., Negative; N.S., non-significant; mPFC, medial prefrontal cortex; PCC, posterior cingulate cortex; pDMN, posterior DMN; Pos., Positive; ROI, region-of-interest; rtfMRI-NF, real-time fMRI neurofeedback; SMS_S, short version of the State Mindfulness Scale; TPF, task-performance feedback. Detailed information about outliers, *p*-value correction of correlation coefficient (i.e., *r*), confidence interval (CI), and stratified scenarios of statistical significance is presented in Table 3.

4.5. Time-course of regression coefficient from mediation analysis compared with FC from the Pearson's and partial correlation analyses

Increased FC levels between the SN and the DMN were observed in participants with relatively short mindfulness training experience (Mooneyham et al., 2016). Based on the results of our mediation analysis, time-points that showed statistically greater slope levels from the experimental group than the control group were more evident compared to when using Pearson's correlation or partial correlation analyses (Fig. 5 vs. Fig. 8). These results indicate that our analysis model of the mediation of the triple networks may be better suited to describe our experimental data than the two alternative analysis models. Interestingly, the significantly increased slope levels between the SN and the DMN, as mediated by the CEN, in the transfer run at the beginning of the run from 90 s to about 105 s were more noticeable for the experimental group than the control group (Fig. 5a). This may be because of the rehearsal of the mindfulness strategy just before the 300 s task-period (Fig. 1b), indicating that only the participants from the experimental group had successfully learned how to employ the mindfulness strategy with the assistance of the two rtfMRI-NF runs.

4.6. Alternative mediation analysis model of the triple networks in comparison with Pearson's correlation and partial correlation analyses

Although our results seem to indicate that our hypothesized regression coefficient (i.e., slope) from the SN to the DMN, as mediated by the CEN, is a strong candidate for the feature of mindfulness, it is also worth noting that the slope level from the DMN to the SN, as mediated by the CEN, has also shown weakly suggestive positive correlations with the mindfulness/task-performance scores in the rtfMRI-NF runs only in the experimental group (Fig. S4). This slope level of the experimental group also showed a potentially weakly suggestive positive correlation with the mindfulness scores in the transfer run. Interestingly, for the experimental group the regression coefficients from the DMN to the CEN presented weakly suggestive negative correlations with the mindfulness/task-performance scores (Fig. S5b), whereas for the control group the regression coefficients from the CEN to the DMN showed weakly positive correlations with the mindfulness/task-performance scores (Fig. S5). It is less likely that slope levels between the SN and the CEN, as mediated by the DMN, would be related to mindfulness features (Fig. S6). The correlation analyses using FC levels from alternative pairs of the triple networks as obtained by Pearson's correlation or partial correlation

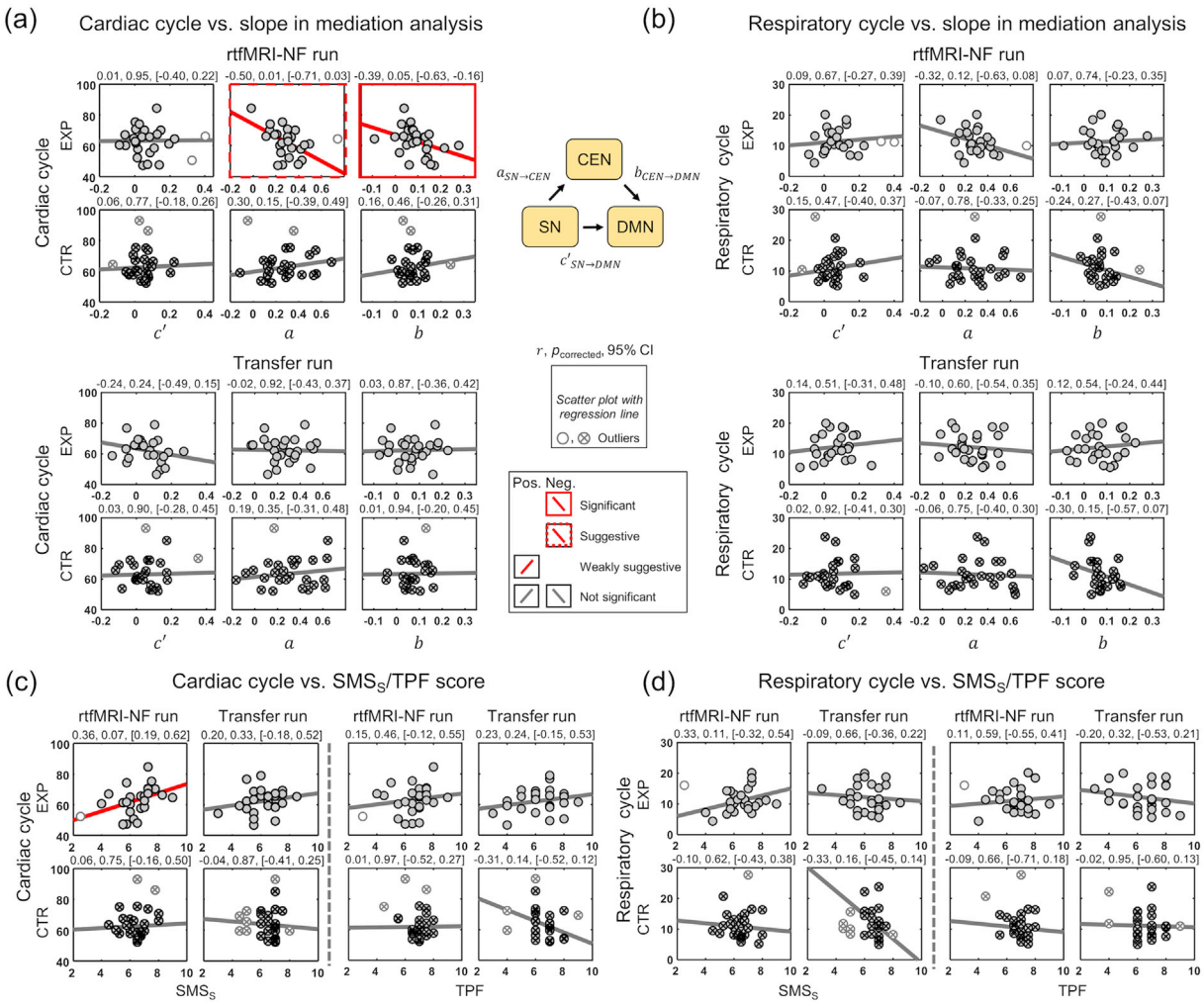

Fig. 11. Scatter plots of the cardiac/respiratory cycles and regression coefficients (or slopes; c', a, b) obtained from the mediation analysis (a–b) and the SMS$_S$/TPF scores (c–d) in the rtfMRI-NF and transfer runs. CEN, central executive network, CTR, control group; DMN, default-mode network; EXP, experimental group; Neg., negative; Pos., positive, rtfMRI-NF, real-time fMRI neurofeedback; SN, salience network; SMS$_S$, short version of the State Mindfulness Scale. Detailed information about outliers, *p*-value correction of correlation coefficient (i.e., *r*), confidence interval (CI), and stratified scenarios of statistical significance is presented in Table 3.

analyses and mindfulness scores did not show significant associations, indicating that these features may not be well suited to our experimental data (Fig. S7).

4.7. Control analyses to investigate the effect of a potential "dual-task" experimental setup

4.7.1. Correlation analysis between paired participants for each of the reported mindfulness/task-performance scores and c' values

Our adopted paradigm may be vulnerable to a potential "dual-effect", in that participants were told to increase the neurofeedback signal c' while enhancing their mindfulness status and subsequently the efficacy of our rtfMRI-NF training was evaluated based on the correlation between c' and mindfulness scores. We observed that (a) there was no meaningful correlation of the mindfulness scores, task-performance feedback scores or c' values between the paired participants across the two groups (Fig. 9) and (b) the activations in the DMN areas also showed a significant negative correlation with mindfulness scores only in the experimental group (Fig. 10). These observations suggest the possibility of modulation of the mindfulness related features of the brain other than that represented by the regression coefficient (i.e., c') from the SN to the DMN, as mediated by the CEN, possibly including the activations in the mPFC and/or PCC.

4.7.2. Association between activations in the default-mode network and mindfulness scores

It is interesting to note that associations between the activations in the DMN and the mindfulness/task-performance scores were significant only for the experimental group, although the statistical significance was less strong than the degree of association between the regression coefficients (i.e., slopes; c') and mindfulness/task-performance scores. In detail, the aDMN and mPFC showed significant negative correlation in the rtfMRI-neurofeedback runs only, whereas the PCC showed significant negative correlation in the transfer run. This might be due to the slightly different functions of the sub-regions of the DMN (Brewer et al., 2011; Garrison et al., 2013; Posner et al., 2007; Tang et al., 2015). More specifically, the aDMN including the mPFC has been reported to be associated with the self-referential processing related to attentional control (Farb et al., 2007; Ives-Deliperi et al., 2011) and the regulation of internal/external attentional sources (Brewer et al., 2013; Burgess et al., 2007; Davey et al., 2016; Scheibner et al., 2017). In our study, the mPFC might have been dominantly involved in the rtfMRI-NF runs given the constantly presented thermometer bar. On the other hand, the PCC activations might have been involved with mindfulness in the transfer run, where there was no neurofeedback information. In fact, Scheibner et al. (2017) reported strong deactivation of the PCC during internal attention (mindfulness to breathing sensations) compared to external attention (i.e., mindfulness to external sounds), and perhaps this difference may

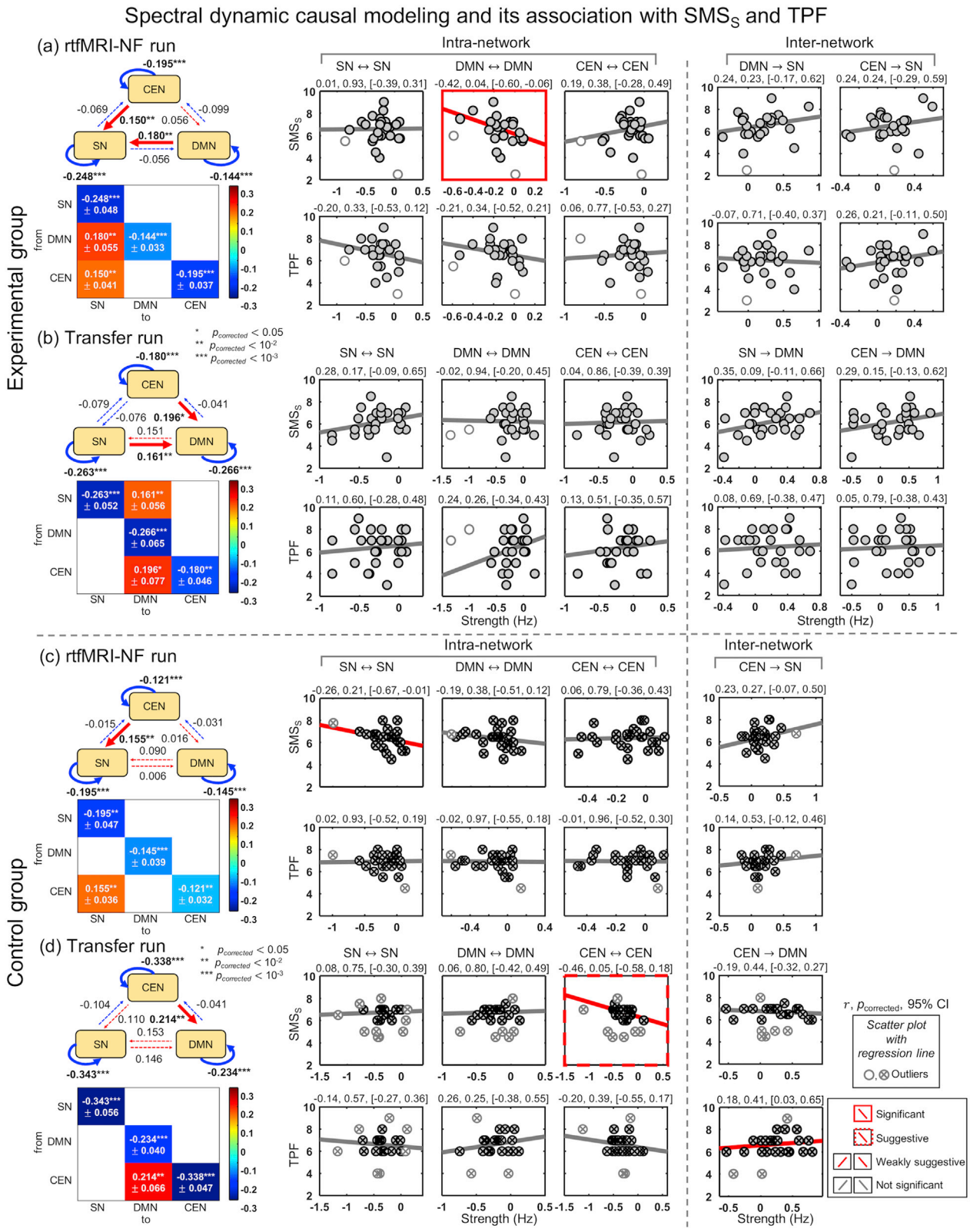

Fig. 12. Spectral dynamic causality modeling (spDCM) results and their association with mindfulness (i.e., SMS_S) and task-performance feedback (TPF) scores across rtfMRI-NF runs and transfer run in the experimental (a–b) and control (c–d) groups. Diagonal elements indicate self-inhibition in log-scale relative to the prior mean of −0.5 Hz (Almgren et al., 2018). Solid lines in red (excitatory connection) and blue (inhibitory connection) indicate significance ($p < 0.05$), whereas dashed lines indicate non significance ($p > 0.05$). CEN, central executive network; DMN, default-mode network; rtfMRI-NF, real-time fMRI neurofeedback; SMS_S, short version of the State Mindfulness Scale; SN, salience network. Detailed information about outliers, *p*-value correction of correlation coefficient (i.e., *r*), confidence interval (CI), and stratified scenarios of statistical significance is presented in Table 3.

reflect the internal self-referential processing role of the PCC. Despite these findings, it is still unclear whether (a) the changes in our neurofeedback information (i.e., the c' slope value) were driven by the activation changes from a single ROI or multiple ROIs in the triple networks and/or (b) the changes in our neurofeedback information drove the activation changes of the ROIs, so future studies of these possibilities are warranted.

4.7.3. Cardiac/respiratory cycles vs. regression coefficients in the mediation analysis and/or mindfulness/task-performance scores

Participants in the experimental group may have enhanced their mindfulness status while suppressing a link with any cognitive effort related to the thermometer bar (i.e., the slope *a* from the SN to the CEN and the slope *b* from the CEN to the DMN). Our results showed negative correlation between the cardiac cycles and either *a* or *b* and positive correlation between the cardiac cycles and the mindfulness scores. Previous studies seem to support our findings, in which an increase in cardiac cycles has been associated with increased sympathetic activity of the autonomic nervous system (ANS), which is related to the suppression of external stimuli (Lacey and Lacey, 2017; Laumann et al., 2003). However, a more systematic investigation is warranted to analyze our data in the context of ANS activity, such as by using heart rate variability, which is believed to better reflect the parasympathetic and sympathetic activity of the ANS (Amihai and Kozhevnikov, 2015; Holsen et al., 2011; Krygier et al., 2013; Tang et al., 2009).

4.8. Effective connectivity of the triple networks

The effective connectivity results obtained from our experimental data seem to provide supplemental evidence supporting our hypothesized model of mindfulness in the triple networks framework. For example, the results of the mediation analysis showed that, in the rtfMRI-NF runs, the regression coefficient (i.e., slope) from the SN to the DMN, as mediated by the CEN, presented greater levels of correlation with mindfulness scores and task-performance feedback scores than the slope from the DMN to the SN. Moreover, our effective connectivity analysis also suggested that mindfulness status that is reflected in the DMN (Brewer and Garrison, 2014; Mooneyham et al., 2016; Uddin, 2015) as well as the cognitive control in the CEN (Mooneyham et al., 2016; Seeley et al., 2007) also caused the activations related to the interoceptive perception of the SN (Farb et al., 2013) in the rtfMRI-NF runs. Interestingly, in the transfer run, the SN and CEN caused the activations in the DMN. It is possible that this effective connectivity change was associated with the presence and absence of the neurofeedback interface (i.e., thermometer bar) in the rtfMRI-NF and transfer runs, respectively. On the other hand, with the control group, there was no significant effective connectivity between interoceptive perception (i.e., the SN) and mindfulness status (i.e., the DMN). This finding is consistent with other results on the absence of significant correlations between the regression coefficients (i.e., c') from the SN to the DMN and mindfulness/task-performance scores in the control group. In fact, the potentially positive correlation between inter-network effective connectivity from the CEN to the DMN and the task-performance feedback score in the transfer run of the control group is also consistent with the positive correlations of the control group between regression coefficient *b* in the mediation analysis and the task-performance feedback scores (Fig. 6b). The causal relationships between the triple networks can also be derived from the Granger causality analysis (Cohen Kadosh et al., 2016; Lee et al., 2012c).

4.9. Time spans of rtfMRI-NF training

A number of other studies have also reported a training effect guided by rtfMRI-NF within the relatively short training time of a single day (deCharms et al., 2005; Emmert et al., 2016; Haller et al., 2010; Kim et al., 2015a; Lee et al., 2009, 2012c; Marins et al., 2015; Perronnet et al., 2017; Yoo and Jolesz, 2002; Yoo et al., 2007, 2008; Young et al., 2014; Zotev et al., 2011, 2014). For example, in one of the seminal papers on rtfMRI-NF by deCharms et al. (2005), each run consisted of five blocks (1 min/block) for each of the up-regulation and down-regulation phases of activation in the rostral anterior cingulate cortex (rACC) area, which has been related to chronic pain perception (deCharms et al., 2005) and an increase in the rACC BOLD signals was observed in the second rtfMRI-NF training run. In a series of studies employing rtfMRI-NF training for the amygdala activation by happy memory retrieval (Young et al., 2014; Zotev et al., 2011, 2014), there were three runs of rtfMRI-NF training each featuring four blocks of happy memory retrieval training (40 s/block; 2 min 40 s/run; 8 min across the three runs) and an increase in the amygdala activation across these three rtfMRI-NF training runs was reported. In the study by Haller et al. (2010), in each of four rtfMRI-NF training runs, there was a period of about 2 min for participants having chronic tinnitus to learn the down-regulation of auditory activations, with the rtfMRI-NF training period totaling approximately 8 min. Using motor imagery as a target task strategy, increased activations in the motor areas have been reported after approximately 10 min of rtfMRI-NF training (Marins et al., 2015; Perronnet et al., 2017). In the meta-analysis of Emmert et al. (2016), several other studies were reported to have used an overall rtfMRI-NF training length of less than approximately 10 min (for example, Berman et al. (2013), Sulzer et al. (2013), and Veit et al. (2012) (Berman et al., 2013; Emmert et al., 2016; Sulzer et al., 2013b; Veit et al., 2012)).

There have also been other rtfMRI-NF studies that were conducted across several days of training sessions (Scharnowski et al., 2015; Sherwood et al., 2016). For example, Scharnowski et al. (2015) reported that participants learned to up- and down-regulate the BOLD signal defined as the difference between the BOLD signals in the supplementary motor area and parahippocampal place area, by controlling motor- and memory-related activation (Scharnowski et al., 2015). In this study, participants took about 12–22 runs (i.e., three 45 s up-regulation blocks and three 45 s down-regulation blocks in one run) across 4–6 days to learn a significant level of self-regulation. Also, Sherwood et al. (2016) reported that participants took five rtfMRI-NF sessions across two weeks (16 min total; each session consisted of one run; four 48 s blocks/run, or 3 min 12 s/run) to learn to up regulate working memory performance based on the BOLD signal in the dorsolateral prefrontal cortex (Sherwood et al., 2016).

It is also important to note that rtfMRI-NF training methods using indirect and/or covert information transformed from brain data as a neurofeedback signals tend to adopt a prolonged training period (Ramot et al., 2016; Shibata et al., 2011). For example, Ramot et al. (2016) reported that each participant performed five consecutive rtfMRI-NF runs (10 min/run) per day across 5 separate days to learn to regulate the differential activation of two category-selective visual perception areas (i.e., fusiform area and parahippocampal place area) via covert neurofeedback information (i.e., reward) (Ramot et al., 2016). In the study by Shibata et al. (2011), rtfMRI-NF training to learn the induction of activation patterns in the early visual cortex was conducted during 5 or 10 days using the information from a pre-trained fMRI decoder. Across subjects and days, an average of 10.8 runs of rtfMRI-NF training (5 min/run) was conducted in each day (Shibata et al., 2011). It would be an interesting meta-analysis study to systematically investigate the time span of rtfMRI-NF training depending on whether the neurofeedback information was comprised of direct/overt information (i.e., brain activation and connectivity) or indirect/covert information (e.g., reward and/or decoded information).

4.10. Strength of the study, potential weakness, and future works

One major strength of our study was that we evaluated potential functional features of mindfulness using independently measured mindfulness scores by systematically changing the mediation analysis

models of the triple networks. In addition, our results from Pearson's correlation and partial correlation analyses were compared with the results from the mediation analysis to further justify the partial regression coefficient (i.e., slope) level from the SN to the DMN, as mediated by the CEN, being one of the functional features of mindfulness in our experimental setting.

Precautions were taken to ensure that the experimenters and participants were blind to the group assignment. Notwithstanding, the experimenter who developed our rtfMRI-NF software toolbox and executed the software during the MRI session (i.e., first author of this paper) was aware of the group assignment of the participants so that he could properly operate the software toolbox on MRI session day since the neurofeedback information of the participants in the control group had to be substituted with the neurofeedback information of their paired participants in the experimental group. However, it is important to note that this experimenter, who also performed the data analyses, did not collect any of the subjective ratings in the pre- and post-MRI sessions. Instead, other staff members (S.J., J.L., and D.-Y. K. of co-authors) who were blinded to the assignment interviewed and collected the questionnaires from the participants. Also, the SMS_S and TPF scores obtained from the rtfMRI-NF training runs and transfer runs (Fig. 1b) were automatically recorded via our software toolbox without any interaction with the participants.

The initial ROIs of the triple networks were fine-tuned in individual native EPI space by applying ICA to two concatenated 3-min resting-state blocks (Beckmann and Smith, 2004) based on an independence assumption across spatial patterns (i.e., spatial ICA) (McKeown et al., 1998a). The spatial patterns from the spatial ICA have had their reproducibility and/or reliability demonstrated across different sessions/runs and different tasks (Calhoun et al., 2008; Damoiseaux et al., 2006; De Luca et al., 2006; Mennes et al., 2010; Van Den Heuvel and Pol, 2010; Zuo et al., 2010). For example, Calhoun et al. (2008) reported that the spatial patterns obtained from the spatial ICA were preserved overall across an auditory oddball task and resting-state periods (Calhoun et al., 2008). Thus, we believe that our extracted spatial patterns of the triple networks taken during the resting-state blocks would not be subject to a critical confounding effect from the preceding tasks (i.e., mindfulness, mind-wandering, and/or three cognitive tasks). Nonetheless, it is worth noting the possibility of a potential residual/confounding effect from the preceding tasks affecting the resting-state blocks, particularly in the time courses of the spatial patterns (Albert et al., 2009; Gordon et al., 2014; Tung et al., 2013).

Considering the distinct functions of the subdivisions of the insula (Uddin, 2015), the ROI of the SN may need to be fine-tuned further to include only its right dorsal anterior insular cortex, known as the 'causal hub' of the SN, which influences other large-scale brain networks, including the CEN and DMN (Sridharan et al., 2008). In addition, further study is warranted to determine whether our rtfMRI-NF-based mindfulness training also alters FC changes between the subnetworks of the DMN (Mooneyham et al., 2016). In order to deploy mindfulness training via EEG based neurofeedback, an important future work would be to investigate the EEG features of mindfulness, such as the rhythmic activities of our EEG data, which was simultaneously acquired with fMRI (Kim et al., 2015b; Tsuchimoto et al., 2017).

In addition, it is possible that the neuronal circuitry of mindfulness may involve brain networks other than the triple networks which were scrutinized in our study. To accommodate such scenarios, the development of a model that can handle more than three networks is necessary. For example, machine learning approaches, including deep neural networks, may be gainfully utilized to extract the representative functional features of mindfulness from the FC levels obtained from all possible combinatorial pairs of brain networks, such as in the automated anatomical labeling atlas (Jang et al., 2017; Kim et al., 2016). In this context, applying machine learning approaches to our non-rtfMRI data acquired during mindfulness and mind-wandering, such as to classify the task type and/or to predict the behavioral score (Kim et al., 2019) is an important future work.

It is unlikely that the sequence-of-condition during ambulatory training (i.e., mindfulness on the first day and mind-wandering on the second day and so on, MF ⇄ MW, or vice versa, MW ⇄ MF) affects the results of the rtfMRI-NF effect reported in our study. This is because there was no main effect of the sequence-of-condition in (a) the PSS, MDMQ, SMS, VAS, and TPF scores obtained on the last day of ambulatory training and (b) the MDMQ, SMS, and VAS scores obtained in the pre-MRI session. The interaction between the group and the sequence-of-condition using the TPF scores is interesting (Fig. S1c). However, these results using the stratified sub-group based on the sequence-of-condition during ambulatory training need careful interpreted since (i) there were an unequal number of subjects (Table 2) which might potentially lead to a biased result and (ii) there was a limited number of participants ($n = 10$; sometimes 9 due to an outlier participant amongst the scores) for the MW ⇄ MF condition in the control group. It is interesting that there seems to be an effect from ambulatory training over time, particularly on the MDMQ calm-nervous scores and mindfulness scores. Future study is warranted to systematically investigate whether the smartphone-based ambulatory training conducted as a part of our study was efficient as an intervention tool to improve mood (Meinlschmidt et al., 2016) and whether prolonged longitudinal ambulatory training consolidates the potential learning effect (Garrison et al., 2015; Mason et al., 2018; Noone and Hogan, 2018).

Mediation analysis using the triple networks appears to be well suited to our rtfMRI-NF experimental setup, in which the SN is associated with multisensory interoception (i.e., focused attention to the physical sensations of breathing), the DMN is related to the endogenous event (i.e., the self-referential perception of mindfulness), and the CEN is linked to the exogenous event (i.e., the changing thermometer bar). Although this triple network model of mindfulness appeared to be less-fitted to our data collected during the transfer run when there was no thermometer bar (i.e., Fig. 5b), the effective connectivity analysis suggested that the CEN had the causal effect to the DMN in the transfer run (i.e., Fig. 12b). This indicates that the CEN may also be involved when the mindfulness strategy is employed without a thermometer bar, possibly to reduce distracting thoughts involving cognitive processes (i.e., mind-wandering) that would otherwise interfere with the self-referential perception of mindfulness. Thus, whether our mediation analysis model using the triple networks is also well suited to naturalistic scenarios of mindfulness meditation outside of MRI and without neurofeedback information is an interesting question. In this context, a longitudinal study to acquire fMRI data from mindfulness-meditation-naïve subjects across multiple timepoints during the course of mindfulness training in a naturalistic condition (i.e., outside of an MRI) is warranted. This type of study would serve to evaluate whether prolonged mindfulness training leads to an enhancement of mindfulness status and whether this enhancement is reflected in the functional features of mindfulness.

In our study, attention focused on the physical sensations of breathing was adopted as a mindfulness strategy, and mindfulness-meditation-naïve individuals participated in this cross-sectional study. However, a variety of alternative mindfulness practices exist, including open-monitoring practices, as well as various methodological designs such as a longitudinal study (Rance et al., 2018) and/or comparing results between expert meditators and either non-meditator controls, beginning meditators, or less experienced meditators (Mooneyham et al., 2016). An important research question to answer is whether our presented method and the proposed partial regression coefficient feature of mindfulness can provide converging evidence on the mindful brain across all these diverse mindfulness scenarios.

5. Conclusions

In this study, we presented a potential functional feature of mindfulness (i.e., the partial regression coefficient from the SN to the DMN, as mediated by the CEN, modeled by mediation analysis of the triple networks) from mindfulness-meditation-naïve participants. In addition, we

Table 2
Sociodemographic information and psychological traits of the participants included in the analyses from the stratified sub-groups based on the sequence-of-condition during the ambulatory training for each of the experimental and control groups.

Categorical Variable	Category	Experimental group (n)		Control group (n)		Total (n)
		MF ⇄ MW ($n = 13$)	MW ⇄ MF ($n = 13$)	MF ⇄ MW ($n = 16$)	MW ⇄ MF ($n = 10$)	
Marital status	Single	11	13	12	9	45
	In a relationship	2	0	4	1	7
Highest degree	High school diploma or equivalent degree	10	11	14	6	41
	Bachelor's degree	1	2	2	4	9
	Master's degree	2	0	0	0	2
Size of household	1	1	2	2	0	5
	2	0	0	0	0	0
	3	0	1	3	1	5
	4	10	7	9	8	34
	5	2	3	2	1	8

Continuous variable	Experimental group (n)		Control group (n)		Two-way ANOVA (F; p from main effect of group, main effect of sequence-of-condition, interaction)
	MF ⇄ MW ($n = 13$)	MW ⇄ MF ($n = 13$)	MF ⇄ MW ($n = 16$)	MW ⇄ MF ($n = 10$)	
Age (years)	25.69 ± 3.84	24.92 ± 2.60	24.75 ± 2.11	25.80 ± 3.22	$F(1,48) = 0.50, 0.09, 2.58$; $p = 0.49, 0.77, 0.12$
Full time education (years)	15.23 ± 2.17	14.46 ± 1.76	14.31 ± 1.20	15.60 ± 1.17	$F(1,48) = 0.00, 0.42, 0.00$; $p = 1.00, 0.52, 1.00$
EHI	95.09 ± 6.15	94.51 ± 7.14	95.01 ± 5.24	94.75 ± 6.72	$F(1,48) = 0.04, 0.02, 0.01$; $p = 0.85, 0.90, 0.95$
BFI-10					
Extraversion	3.31 ± 1.09	3.46 ± 0.72	3.28 ± 1.17	2.85 ± 0.67	$F(1,48) = 1.13, 0.82, 0.05$; $p = 0.29, 0.37, 0.83$
Agreeableness	3.23 ± 0.78	3.04 ± 0.75	3.56 ± 0.75	3.50 ± 0.67	$F(1,48) = 3.78, 0.17, 0.26$; $p = 0.06, 0.68, 0.62$
Conscientiousness	2.88 ± 1.00	3.42 ± 0.70	2.94 ± 0.77	3.25 ± 0.48	$F(1,48) = 0.31, 0.82, 0.05$; $p = 0.58, 0.37, 0.82$
Neuroticism	3.08 ± 0.86	3.19 ± 0.90	2.91 ± 0.95	3.05 ± 0.93	$F(1,48) = 0.64, 0.03, 1.44$; $p = 0.43, 0.87, 0.24$
Openness to Experience	3.81 ± 0.69	3.58 ± 0.73	3.50 ± 0.98	3.65 ± 0.97	$F(1,48) = 0.68, 3.58, 0.06$; $p = 0.42, 0.07, 0.81$
PHQ-9	2.46 ± 2.06	1.08 ± 1.04	2.32 ± 1.40	2.10 ± 1.45	$F(1,47) = 0.77, 0.01, 0.81$; $p = 0.39, 0.97, 0.78$
MAAS	4.78 ± 0.62	4.42 ± 0.46	4.67 ± 0.60	4.71 ± 0.56	$F(1,48) = 0.65, 0.09, 1.43$; $p = 0.42, 0.77, 0.25$
PSS	13.46 ± 4.68	14.54 ± 3.97	12.97 ± 3.75	14.20 ± 3.55	$F(1,48) = 0.29, 0.15, 0.34$; $p = 0.59, 0.70, 0.56$
VAS	3.58 ± 2.11	3.83 ± 1.96	3.28 ± 1.50	4.85 ± 1.89	$F(1,47) = 0.41, 0.15, 0.04$; $p = 0.52, 0.71, 0.85$

$n = 52$ subjects; 8 out of 60 subjects were excluded due to head motion in the two real-time fMRI neurofeedback runs or the transfer run (average frame-wise displacement (FD) > 0.5). Two-way analysis-of-variance (ANOVA) comparing group (experimental group or control group) and sequence-of-condition (MF ⇄ MW or MW ⇄ MF) was conducted (see the "***Analysis of the behavioral data obtained by the smartphone-based ambulatory training***" in the Supplementary Materials for details). One experimental subject who conducted the ambulatory training under the MF⇄ MW cycle was identified as an outlier based on the MAD approach regarding both PHQ-9 and VAS.

BFI, Big Five Inventory-10 (John et al., 1991); EHI, Edinburg Handedness Inventory (Oldfield, 1971); MAAS, Mindful Attention Awareness Scale (Brown and Ryan, 2003); MF, mindfulness; MW, mind-wandering; PHQ, Patient Health Questionnaire (Spitzer et al., 1999); PSS, Perceived Stress Scale (Cohen et al., 1983); VAS, Visual Analog scale for Stress perception (0 being not stressed at all, 10 being extremely stressed).

Table 3
Summary of the statistical significance stratified based on both p-value from a random permutation[a] and confidence interval (CI) from bootstrapping[b] after the exclusion of potential outliers[c]. Unlike a previous approach (Terhune et al., 2014), a "potentially weakly suggestive" was also considered when the CIs did not include a small positive value $\varepsilon \triangleq 0.05$ $-\varepsilon$ even though 0 was in the CIs.

	$0 \notin CI$	$0 \in CI$	
$p \leq 0.05$	Significant	Suggestive	
$p > 0.05$	Weakly suggestive	$\varepsilon \notin CI$ *or* $-\varepsilon \notin CI$	$\varepsilon \in CI$ *or* $-\varepsilon \in CI$
		Potentially weakly suggestive	Not significant

[a] Total of 10,000 random permutations using randomized indices of participants were conducted and the p-value was obtained from the corresponding null distribution (Groppe et al., 2011; Manly, 2006).

[b] The 95% confidence interval (CI) of correlation coefficients was obtained from 10,000 cycles of bootstrapping with replacement (Pernet et al., 2013; Terhune et al., 2014).

[c] Refer to the section, "***Definition of outliers based on median absolute deviation (MAD)***" in the Supplemental Material for details.

demonstrated the possibility of enhancing this functional feature via rtfMRI-NF-based mindfulness training. The validity of this functional feature of mindfulness was systematically evaluated using independently measured subjective ratings of mindfulness scores, and by comparing alternative FC levels in the triple networks obtained by Pearson's correlation and partial correlation analyses. Since the triple networks can model aberrant saliency mapping and cognitive dysfunction across a span of mental and neurological disorders (Menon, 2011), as well as the typical development of the human brain (Uddin et al., 2011) and emotion (Touroutoglou et al., 2015; Young et al., 2017), the presented mediation analysis model across the triple networks may be a viable tool widely applicable to the treatment of mental and neurological disorders using rtfMRI-NF training.

Conflicts of interest

The authors have no conflicts of interest regarding this study, including financial, consultant, institutional, or other relationships. GM was a consultant for Janssen Research & Development, LLC. The sponsors had no involvement in the study design, data collection, analysis or interpretation of data, manuscript preparation, or the decision to submit for publication.

Funding

This work was supported by the National Research Foundation (NRF) grant, MSIP of Korea (NRF-2017R1E1A1A01077288, NRF-2016M3C7A1914450), in part by the National Research Council of Science & Technology (NST) grant by the Korea government (MSIT) [No. CAP-18-01-KIST], in part by the Electronics and Telecommunications Research Institute (ETRI) grant funded by the Korean government. [19ZS1100], and in part by the Korean Health Technology R&D Project, Ministry of Health & Welfare, Korea (HI12C1847).

Acknowledgements

Authors would like to thank Ms. Da-Woon Heo for her logistic support during the data collection and Mr. Niv Lustig for his edits.

Appendix

Appendix A. Functional connectivity (FC) level from the Pearson's correlation analysis

The Pearson's correlation coefficient can be used to estimate the level of FC between the SN and the DMN as follows (Cohen et al., 2013):

$$c = \frac{\frac{1}{n}\sum_{t=1}^{n}\left[(x(t)-\mu_x)(y(t)-\mu_y)\right]}{\sqrt{\frac{1}{n}\sum_{t=1}^{n}(x(t)-\mu_x)^2}\sqrt{\frac{1}{n}\sum_{t=1}^{n}(y(t)-\mu_y)^2}} = \frac{\sigma_{xy}}{\sigma_x\sigma_y} = r_{xy} \tag{A.1}$$

where $x(t)$ is the BOLD signal of the SN at time t, $y(t)$ is the BOLD signal of the DMN, n is the number of time points (i.e., TRs) in the BOLD signal, r_{xy} is the Pearson's correlation coefficient between $x(t)$ and $y(t)$, μ_x and μ_y are the mean values of $x(t)$ and $y(t)$, respectively, σ_{xy} is the covariance between the two variables, and σ_x and σ_y are the standard deviations of $x(t)$ and $y(t)$, respectively.

Appendix B. Regression coefficients (i.e., slopes) from the mediation analysis

In the mediation analysis model of the triple networks (Fig. 2a), the BOLD signal of the DMN, $y(t)$ (i.e., denoted as column vector $\boldsymbol{y}$; dependent variable) can be represented as a linear summation of the BOLD signal of the SN, $x(t)$ (i.e., denoted as column vector $\boldsymbol{x}$; independent variable) and the BOLD signal of the CEN, $m(t)$ (i.e., denoted as column vector $\boldsymbol{m}$; mediator variable) (MacKinnon et al., 2007):

$$\boldsymbol{y} = c'\boldsymbol{x} + b\boldsymbol{m} + b_1 + \boldsymbol{e}_1 \tag{A.2}$$

where c' and b are the regression coefficients (i.e., slopes) for predicting $\boldsymbol{y}$ using the predictors $\boldsymbol{x}$ and $\boldsymbol{m}$, respectively, b_1 is a bias term to adjust for the baseline BOLD intensity of $\boldsymbol{y}$, and $\boldsymbol{e}_1$ is the residual. Similarly, the mediator variable $\boldsymbol{m}$ can be represented using the independent variable $\boldsymbol{x}$:

$$\boldsymbol{m} = a\,\boldsymbol{x} + b_2 + \boldsymbol{e}_2 \tag{A.3}$$

where a is the regression coefficient of the predictor $\boldsymbol{x}$, b_2 is a bias term, and $\boldsymbol{e}_2$ is the residual.

From Eqs. (A.2) and (A.3),

$$\boldsymbol{y} = c'\boldsymbol{x} + b(a\,\boldsymbol{x} + b_2 + \boldsymbol{e}_2) + b_1 + \boldsymbol{e}_1 = (c' + ab)\boldsymbol{x} + bb_2 + b_1 + b\boldsymbol{e}_2 + \boldsymbol{e}_1 = c\boldsymbol{x} + b_3 + \boldsymbol{e}_3 \tag{A.4}$$

where $c\ (= c' + ab)$ is the regression coefficient (i.e., total effect) from the predictor $\boldsymbol{x}$ to the response variable $\boldsymbol{y}$, b_3 is a bias term, and $\boldsymbol{e}_3$ is the residual.

Eq. (A.2) is equivalent to the following equation:

$$\boldsymbol{y}_0 = [\boldsymbol{x}_0 \quad \boldsymbol{m}_0]\begin{bmatrix} c' \\ b \end{bmatrix} + \tilde{\boldsymbol{e}}_1 \tag{A.5}$$

where $\boldsymbol{y}_0, \boldsymbol{x}_0$, and $\boldsymbol{m}_0$ are the zero-meaned $\boldsymbol{y}$, $\boldsymbol{x}$, and $\boldsymbol{m}$, respectively, and $\tilde{\boldsymbol{e}}_1$ is the residual from the zero-meaned variables. Applying the least-squares (LS) algorithm to Eq. (A.5):

$$\begin{bmatrix} c' \\ b \end{bmatrix} = \left([\boldsymbol{x}_0 \quad \boldsymbol{m}_0]^T[\boldsymbol{x}_0 \quad \boldsymbol{m}_0]\right)^{-1}[\boldsymbol{x}_0 \quad \boldsymbol{m}_0]^T\boldsymbol{y}_0 = \begin{bmatrix} \boldsymbol{x}_0^T\boldsymbol{x}_0 & \boldsymbol{x}_0^T\boldsymbol{m}_0 \\ \boldsymbol{m}_0^T\boldsymbol{x}_0 & \boldsymbol{m}_0^T\boldsymbol{m}_0 \end{bmatrix}^{-1}\begin{bmatrix} \boldsymbol{x}_0^T\boldsymbol{y}_0 \\ \boldsymbol{m}_0^T\boldsymbol{y}_0 \end{bmatrix} \tag{A.6}$$

Now, $\boldsymbol{x}_0^T\boldsymbol{x}_0 = \sigma_x^2$, $\boldsymbol{m}_0^T\boldsymbol{m}_0 = \sigma_m^2$, $\boldsymbol{x}_0^T\boldsymbol{m}_0 = \boldsymbol{m}_0^T\boldsymbol{x}_0 = r_{xm}\sigma_x\sigma_m$, $\boldsymbol{x}_0^T\boldsymbol{y}_0 = r_{xy}\sigma_x\sigma_y$, $\boldsymbol{m}_0^T\boldsymbol{y}_0 = r_{my}\sigma_m\sigma_y$, where σ_i is the standard deviation of the variable i and r_{ij} is the Pearson's correlation coefficient between variables i and j. Thus, the LS solution in Eq. (A.6) becomes:

$$c' = \frac{r_{xy} - r_{xm}r_{my}}{1 - r_{xm}^2}\frac{\sigma_y}{\sigma_x},\quad b = \frac{r_{my} - r_{xy}r_{xm}}{1 - r_{xm}^2}\frac{\sigma_y}{\sigma_m} \tag{A.7}$$

Similarly, from the LS solution of Eq. (A.3):

$$a = r_{xm}\frac{\sigma_m}{\sigma_x} \tag{A.8}$$

Appendix C. Comparison between the mediation analysis and partial correlation analysis

The partial correlation coefficient can be used to estimate the level of FC between the SN and DMN with an adjusting variable from the CEN as follows (Cohen et al., 2013):

$$r_{xy \cdot m} = \frac{r_{xy} - r_{xm} r_{my}}{\sqrt{\left(1 - r_{xm}^2\right)\left(1 - r_{my}^2\right)}} \tag{A.9}$$

Now, let's suppose the two scenarios of no mediation effect (i.e., $ab = 0$, when $a = 0$ or $b = 0$):

(i) When $a = 0$ (i.e., $r_{xm} = 0$):

$$c' = r_{xy}\frac{\sigma_y}{\sigma_x} (= c;\ \therefore \text{same as the total effect}) \tag{A.10}$$

$$r_{xy \cdot m} = \frac{r_{xy}}{\sqrt{\left(1 - r_{my}^2\right)}} \left(\geq r_{xy};\ \therefore \text{greater than or equal to the simplecorrlection}\right) \tag{A.11}$$

(ii) When b = 0 (i.e., $r_{my} = r_{xy} r_{xm}$):

$$c' = \frac{r_{xy} - r_{xm} r_{my}}{1 - r_{xm}^2}\frac{\sigma_y}{\sigma_x} = r_{xy}\frac{\sigma_y}{\sigma_x}\ (= c;\ \therefore \text{same as the total effect}) \tag{A.12}$$

$$r_{xy \cdot m} = \frac{r_{xy} - r_{xm} r_{my}}{\sqrt{\left(1 - r_{xm}^2\right)\left(1 - r_{my}^2\right)}} = r_{xy}\frac{\sqrt{\left(1 - r_{xm}^2\right)}}{\sqrt{\left(1 - r_{xy}^2\, r_{xm}^2\right)}} \left(\leq r_{xy};\ \therefore \text{smaller than or equal to the simple correlation}\right) \tag{A.13}$$

In summary, when there is no mediation effect, the direct effect (i.e., c') is the same as the total effect (i.e., c) whereas the partial correlation coefficient (i.e., $r_{xy \cdot m}$) is not always the same as the simple correlation coefficient (i.e., r_{xy}). Therefore, the partial correlation coefficient cannot inform the mediation effect.

Now, let's suppose that the simple correlation between the independent variable and mediator variable (i.e., r_{xm}) is the same as the simple correlation between the mediator variable and dependent variable (i.e., r_{my}), i.e., $r_{xm} = r_{my}$. From Eqs. (A.7) and (A.9),

$$c' = \frac{r_{xy} - r_{xm}^2}{1 - r_{xm}^2}\frac{\sigma_y}{\sigma_x} = r_{xy \cdot m}\frac{\sigma_y}{\sigma_x} \tag{A.14}$$

Thus, the direct effect between the independent variable and dependent variable is the same as the partial correlation coefficient when these variables are standardized.

Appendix A. Supplementary data

Supplementary data to this article can be found online at https://doi.org/10.1016/j.neuroimage.2019.03.066.

References

Albert, N.B., Robertson, E.M., Miall, R.C., 2009. The resting human brain and motor learning. Curr. Biol. 19, 1023–1027.

Allen, E.A., Damaraju, E., Plis, S.M., Erhardt, E.B., Eichele, T., Calhoun, V.D., 2014. Tracking whole-brain connectivity dynamics in the resting state. Cerebr. Cortex 24, 663–676.

Almgren, H., Van de Steen, F., Kuhn, S., Razi, A., Friston, K., Marinazzo, D., 2018. Variability and reliability of effective connectivity within the core default mode network: a multi-site longitudinal spectral DCM study. Neuroimage 183, 757–768.

Amihai, I., Kozhevnikov, M., 2015. The influence of buddhist meditation traditions on the autonomic system and attention. BioMed Res. Int. 2015.

Baer, R.A., 2003. Mindfulness training as a clinical intervention: a conceptual and empirical review. Clin. Psychol. Sci. Pract. 10, 125–143.

Barrett, L.F., Simmons, W.K., 2015. Interoceptive predictions in the brain. Nat. Rev. Neurosci. 16, 419.

Beaty, R.E., Benedek, M., Kaufman, S.B., Silvia, P.J., 2015. Default and executive network coupling supports creative idea production. Sci. Rep. 5, 10964.

Beckmann, C.F., Smith, S.M., 2004. Probabilistic independent component analysis for functional magnetic resonance imaging. IEEE Trans. Med. Imaging 23, 137–152.

Behzadi, Y., Restom, K., Liau, J., Liu, T.T., 2007. A component based noise correction method (CompCor) for BOLD and perfusion based fMRI. Neuroimage 37, 90–101.

Berman, B.D., Horovitz, S.G., Hallett, M., 2013. Modulation of functionally localized right insular cortex activity using real-time fMRI-based neurofeedback. Front. Hum. Neurosci. 7, 638.

Bilevicius, E., Smith, S.D., Kornelsen, J., 2018. Resting-state network functional connectivity patterns associated with the mindful attention awareness scale. Brain Connect. 8, 40–48.

Birn, R.M., Murphy, K., Bandettini, P.A., 2008. The effect of respiration variations on independent component analysis results of resting state functional connectivity. Hum. Brain Mapp. 29, 740–750.

Bressler, S.L., Menon, V., 2010. Large-scale brain networks in cognition: emerging methods and principles. Trends Cognit. Sci. 14, 277–290.

Brewer, J., Garrison, K., Whitfield-Gabrieli, S., 2013. What about the "self" is processed in the posterior cingulate cortex? Front. Hum. Neurosci. 7, 647.

Brewer, J.A., Garrison, K.A., 2014. The posterior cingulate cortex as a plausible mechanistic target of meditation: findings from neuroimaging. Ann. N. Y. Acad. Sci. 1307, 19–27.

Brewer, J.A., Worhunsky, P.D., Gray, J.R., Tang, Y.-Y., Weber, J., Kober, H., 2011. Meditation experience is associated with differences in default mode network activity and connectivity. Proc. Natl. Acad. Sci. Unit. States Am. 108, 20254–20259.

Brown, K.W., Ryan, R.M., 2003. The benefits of being present: mindfulness and its role in psychological well-being. J. Personal. Soc. Psychol. 84, 822.

Burgess, P.W., Dumontheil, I., Gilbert, S.J., 2007. The gateway hypothesis of rostral prefrontal cortex (area 10) function. Trends Cognit. Sci. 11, 290–298.

Calhoun, V.D., Kiehl, K.A., Pearlson, G.D., 2008. Modulation of temporally coherent brain networks estimated using ICA at rest and during cognitive tasks. Hum. Brain Mapp. 29, 828–838.

Chai, X.J., Castanon, A.N., Ongur, D., Whitfield-Gabrieli, S., 2012. Anticorrelations in resting state networks without global signal regression. Neuroimage 59, 1420–1428.

Christoff, K., Irving, Z.C., Fox, K.C., Spreng, R.N., Andrews-Hanna, J.R., 2016. Mind-wandering as spontaneous thought: a dynamic framework. Nat. Rev. Neurosci. 17, 718.

Cohen, J., Cohen, P., West, S.G., Aiken, L.S., 2013. Applied Multiple Regression/correlation Analysis for the Behavioral Sciences. Routledge.

Cohen Kadosh, K., Luo, Q., de Burca, C., Sokunbi, M.O., Feng, J., Linden, D.E.J., Lau, J.Y.F., 2016. Using real-time fMRI to influence effective connectivity in the developing emotion regulation network. Neuroimage 125, 616–626.

Cohen, S., Kamarck, T., Mermelstein, R., 1983. A global measure of perceived stress. J. Health Soc. Behav. 385–396.

Cole, M.W., Repovš, G., Anticevic, A., 2014. The frontoparietal control system: a central role in mental health. Neuroscientist 20, 652–664.

Creswell, J.D., Taren, A.A., Lindsay, E.K., Greco, C.M., Gianaros, P.J., Fairgrieve, A., Marsland, A.L., Brown, K.W., Way, B.M., Rosen, R.K., 2016. Alterations in resting-

state functional connectivity link mindfulness meditation with reduced interleukin-6: a randomized controlled trial. Biol. Psychiatry 80, 53–61.
Damoiseaux, J., Rombouts, S., Barkhof, F., Scheltens, P., Stam, C., Smith, S.M., Beckmann, C., 2006. Consistent resting-state networks across healthy subjects. Proc. Natl. Acad. Sci. Unit. States Am. 103, 13848–13853.
Davey, C.G., Pujol, J., Harrison, B.J., 2016. Mapping the self in the brain's default mode network. NeuroImage 132, 390–397.
De Luca, M., Beckmann, C., De Stefano, N., Matthews, P., Smith, S.M., 2006. fMRI resting state networks define distinct modes of long-distance interactions in the human brain. NeuroImage 29, 1359–1367.
deCharms, R.C., Maeda, F., Glover, G.H., Ludlow, D., Pauly, J.M., Soneji, D., Gabrieli, J.D., Mackey, S.C., 2005. Control over brain activation and pain learned by using real-time functional MRI. Proc. Natl. Acad. Sci. U. S. A. 102, 18626–18631.
Diamond, A., Lee, K., 2011. Interventions shown to aid executive function development in children 4 to 12 years old. Science 333, 959–964.
Dickenson, J., Berkman, E.T., Arch, J., Lieberman, M.D., 2013. Neural correlates of focused attention during a brief mindfulness induction. Soc. Cognit. Affect Neurosci. 8, 40–47.
Doll, A., Hölzel, B.K., Boucard, C.C., Wohlschläger, A.M., Sorg, C., 2015. Mindfulness is associated with intrinsic functional connectivity between default mode and salience networks. Front. Hum. Neurosci. 9, 461.
Doll, A., Holzel, B.K., Mulej Bratec, S., Boucard, C.C., Xie, X., Wohlschlager, A.M., Sorg, C., 2016. Mindful attention to breath regulates emotions via increased amygdala-prefrontal cortex connectivity. Neuroimage 134, 305–313.
Dunne, J., 2018. Mindfulness in anorexia nervosa: an integrated review of the literature. J. Am. Psychiatr. Nurses Assoc. 24 (2), 109–117, 1078390317711250.
Emmert, K., Kopel, R., Sulzer, J., Brühl, A.B., Berman, B.D., Linden, D.E., Horovitz, S.G., Breimhorst, M., Caria, A., Frank, S., 2016. Meta-analysis of real-time fMRI neurofeedback studies using individual participant data: how is brain regulation mediated? Neuroimage 124, 806–812.
Fair, D.A., Cohen, A.L., Dosenbach, N.U., Church, J.A., Miezin, F.M., Barch, D.M., Raichle, M.E., Petersen, S.E., Schlaggar, B.L., 2008. The maturing architecture of the brain's default network. Proc. Natl. Acad. Sci. Unit. States Am. 105, 4028–4032.
Farb, N.A., Segal, Z.V., Anderson, A.K., 2013. Mindfulness meditation training alters cortical representations of interoceptive attention. Soc. Cognit. Affect Neurosci. 8, 15–26.
Farb, N.A., Segal, Z.V., Mayberg, H., Bean, J., McKeon, D., Fatima, Z., Anderson, A.K., 2007. Attending to the present: mindfulness meditation reveals distinct neural modes of self-reference. Soc. Cognit. Affect Neurosci. 2, 313–322.
Friston, K.J., Kahan, J., Biswal, B., Razi, A., 2014. A DCM for resting state fMRI. Neuroimage 94, 396–407.
Froeliger, B., Garland, E.L., Kozink, R.V., Modlin, L.A., Chen, N.-K., McClernon, F.J., Greeson, J.M., Sobin, P., 2012. Meditation-state functional connectivity (msFC): strengthening of the dorsal attention network and beyond. Evid. Based Complement Altern. Med. 2012.
Garrison, K.A., Pal, P., Rojiani, R., Dallery, J., O'Malley, S.S., Brewer, J.A., 2015. A randomized controlled trial of smartphone-based mindfulness training for smoking cessation: a study protocol. BMC Psychiatry vol. 15, 83.
Garrison, K.A., Scheinost, D., Worhunsky, P.D., Elwafi, H.M., Thornhill, T.A., Thompson, E., Saron, C., Desbordes, G., Kober, H., Hampson, M., 2013. Real-time fMRI links subjective experience with brain activity during focused attention. Neuroimage 81, 110–118.
Glover, G.H., Li, T.Q., Ress, D., 2000. Image-based method for retrospective correction of physiological motion effects in fMRI: RETROICOR. Magn. Reson. Med. 44, 162–167.
Gordon, E.M., Breeden, A.L., Bean, S.E., Vaidya, C.J., 2014. Working Memory-related Changes in Functional Connectivity Persist beyond Task Disengagement. Hum. Brain Mapp. 35, 1004–1017.
Grant, D.A., Berg, E., 1948. A behavioral analysis of degree of reinforcement and ease of shifting to new responses in a Weigl-type card-sorting problem. J. Exp. Psychol. 38, 404.
Groppe, D.M., Urbach, T.P., Kutas, M., 2011. Mass univariate analysis of event-related brain potentials/fields I: a critical tutorial review. Psychophysiology 48, 1711–1725.
Haller, S., Birbaumer, N., Veit, R., 2010. Real-time fMRI feedback training may improve chronic tinnitus. Eur. Radiol. 20, 696–703.
Hasenkamp, W., Barsalou, L.W., 2012. Effects of meditation experience on functional connectivity of distributed brain networks. Front. Hum. Neurosci. 6, 38.
Hofmann, S.G., Sawyer, A.T., Witt, A.A., Oh, D., 2010. The effect of mindfulness-based therapy on anxiety and depression: a meta-analytic review. J. Consult. Clin. Psychol. 78, 169.
Holsen, L.M., Spaeth, S.B., Lee, J.-H., Ogden, L.A., Klibanski, A., Whitfield-Gabrieli, S., Goldstein, J.M.J.J.o.a.d., 2011. stress response circuitry hypoactivation related to hormonal dysfunction in women with major depression. J. Affect. Disord. 131, 379–387.
Ives-Deliperi, V.L., Solms, M., Meintjes, E.M., 2011. The neural substrates of mindfulness: an fMRI investigation. Soc. Neurosci. 6, 231–242.
Jang, H., Plis, S.M., Calhoun, V.D., Lee, J.H., 2017. Task-specific feature extraction and classification of fMRI volumes using a deep neural network initialized with a deep belief network: evaluation using sensorimotor tasks. Neuroimage 145, 314–328.
Jeon, J., Lee, W., Lee, S., Lee, W., 2007. A pilot study of reliability and validity of the Korean version of mindful attention awareness scale. Kor. J. Clin. Psychol. 26, 201–212.
John, O.P., Donahue, E.M., Kentle, R.L., 1991. The Big Five Inventory—Versions 4a and 54. University of California, Berkeley, Institute of Personality and Social Research, Berkeley, CA.
Kilpatrick, L.A., Suyenobu, B.Y., Smith, S.R., Bueller, J.A., Goodman, T., Creswell, J.D., Tillisch, K., Mayer, E.A., Naliboff, B.D., 2011. Impact of mindfulness-based stress reduction training on intrinsic brain connectivity. Neuroimage 56, 290–298.
Kim, D.Y., Lee, J.H., 2011. Are posterior default-mode networks more robust than anterior default-mode networks? Evidence from resting-state fMRI data analysis. Neurosci. Lett. 498, 57–62.
Kim, D.Y., Yoo, S.S., Tegethoff, M., Meinlschmidt, G., Lee, J.H., 2015a. The inclusion of functional connectivity information into fMRI-based neurofeedback improves its efficacy in the reduction of cigarette cravings. J. Cogn. Neurosci. 27, 1552–1572.
Kim, H.-C., Bandettini, P.A., Lee, J.-H., 2019. Deep neural network predicts emotional responses of the human brain from functional magnetic resonance imaging. Neuroimage 186, 607–627.
Kim, H.C., Yoo, S.S., Lee, J.H., 2015b. Recursive approach of EEG-segment-based principal component analysis substantially reduces cryogenic pump artifacts in simultaneous EEG-fMRI data. Neuroimage 104, 437–451.
Kim, J., Calhoun, V.D., Shim, E., Lee, J.H., 2016. Deep neural network with weight sparsity control and pre-training extracts hierarchical features and enhances classification performance: evidence from whole-brain resting-state functional connectivity patterns of schizophrenia. Neuroimage 124, 127–146.
Kim, J., Kim, Y.H., Lee, J.H., 2013. Hippocampus-precuneus functional connectivity as an early sign of Alzheimer's disease: a preliminary study using structural and functional magnetic resonance imaging data. Brain Res. 1495, 18–29.
Kim, S., Birbaumer, N., 2014. Real-time functional MRI neurofeedback: a tool for psychiatry. Curr. Opin. Psychiatr. 27, 332–336.
King, A.P., Block, S.R., Sripada, R.K., Rauch, S., Giardino, N., Favorite, T., Angstadt, M., Kessler, D., Welsh, R., Liberzon, I., 2016. Altered default mode network (Dmn) resting state functional connectivity following a mindfulness-based exposure therapy for posttraumatic stress disorder (ptsd) in combat veterans of Afghanistan and Iraq. Depress. Anxiety 33, 289–299.
Krygier, J.R., Heathers, J.A., Shahrestani, S., Abbott, M., Gross, J.J., Kemp, A.H., 2013. Mindfulness meditation, well-being, and heart rate variability: a preliminary investigation into the impact of intensive Vipassana meditation, 89, 305–313.
Lacey, B.C., Lacey, J.I., 2017. Studies of Heart Rate and Other Bodily Processes in Sensorimotor Behavior. Cardiovascular Psychophysiology. Routledge, pp. 538–564.
Laumann, K., Gärling, T., Stormark, K.M.J., 2003. Selective attention and heart rate responses to natural and urban environments. J. Environ. Psychol. 23, 125–134.
Lee, J., Shin, C., Ko, Y.H., Lim, J., Joe, S.H., Kim, S., Jung, I.K., Han, C., 2012a. The reliability and validity studies of the Korean version of the Perceived Stress Scale. Korean J. Psychosomat. Med. 20, 127–134.
Lee, J.H., Kim, D.Y., Kim, J., 2012b. Mesocorticolimbic hyperactivity of deprived smokers and brain imaging. Neuroreport 23, 1039–1043.
Lee, J.H., Kim, J., Yoo, S.S., 2012c. Real-time fMRI-based neurofeedback reinforces causality of attention networks. Neurosci. Res. 72, 347–354.
Lee, J.H., O'Leary, H.M., Park, H., Jolesz, F.A., Yoo, S.S., 2008. Atlas-based multichannel monitoring of functional MRI signals in real-time: automated approach. Hum. Brain Mapp. 29, 157–166.
Lee, J.H., Ryu, J., Jolesz, F.A., Cho, Z.H., Yoo, S.S., 2009. Brain-machine interface via real-time fMRI: preliminary study on thought-controlled robotic arm. Neurosci. Lett. 450, 1–6.
Lee, K.U., Kim, J., Yeon, B., Kim, S.H., Chae, J.H., 2013. Development and standardization of extended ChaeLee Korean facial expressions of emotions. Psychiatr. Inv. 10, 155–163.
Lim, J., Teng, J., Patanaik, A., Tandi, J., Massar, S.A., 2018. Dynamic functional connectivity markers of objective trait mindfulness. Neuroimage 176, 193–202.
Linden, D.E., Turner, D.L., 2016. Real-time functional magnetic resonance imaging neurofeedback in motor neurorehabilitation. Curr. Opin. Neurol. 29, 412.
Lutz, A., Jha, A.P., Dunne, J.D., Saron, C.D., 2015. Investigating the phenomenological matrix of mindfulness-related practices from a neurocognitive perspective. Am. Psychol. 70, 632–658.
MacKinnon, D.P., 2008. Introduction to Statistical Mediation Analysis. Routledge.
MacKinnon, D.P., Fairchild, A.J., Fritz, M.S., 2007. Mediation Analysis. J. Annu. Rev. Psychol. 58, 593–614.
Manly, B.F., 2006. Randomization, Bootstrap and Monte Carlo Methods in Biology. Chapman and Hall/CRC.
Marins, T.F., Rodrigues, E.C., Engel, A., Hoefle, S., Basilio, R., Lent, R., Moll, J., Tovar-Moll, F., 2015. Enhancing motor network activity using real-time functional MRI neurofeedback of left premotor cortex. Front. Behav. Neurosci. 9, 341.
Marusak, H.A., Elrahal, F., Peters, C.A., Kundu, P., Lombardo, M.V., Calhoun, V.D., Goldberg, E.K., Cohen, C., Taub, J.W., Rabinak, C.A., 2018. Mindfulness and dynamic functional neural connectivity in children and adolescents. Behav. Brain Res. 336, 211–218.
Mason, A.E., Jhaveri, K., Cohn, M., Brewer, J.A., 2018. Testing a mobile mindful eating intervention targeting craving-related eating: feasibility and proof of concept. J. Behav. Med. 41, 160–173.
McKeown, M.J., Jung, T.P., Makeig, S., Brown, G., Kindermann, S.S., Lee, T.W., Sejnowski, T.J., 1998a. Spatially independent activity patterns in functional MRI data during the stroop color-naming task. Proc. Natl. Acad. Sci. U. S. A. 95, 803–810.
McKeown, M.J., Makeig, S., Brown, G.G., Jung, T.P., Kindermann, S.S., Bell, A.J., Sejnowski, T.J., 1998b. Analysis of fMRI data by blind separation into independent spatial components. Hum. Brain Mapp. 6, 160–188.
Meinlschmidt, G., Lee, J.-H., Stalujanis, E., Belardi, A., Oh, M., Jung, E.K., Kim, H.-C., Alfano, J., Yoo, S.-S., Tegethoff, M., 2016. Smartphone-based psychotherapeutic micro-interventions to improve mood in a real-world setting. Front. Psychol. 7, 1112.
Mennes, M., Kelly, C., Zuo, X.-N., Di Martino, A., Biswal, B.B., Castellanos, F.X., Milham, M.P., 2010. Inter-individual differences in resting-state functional connectivity predict task-induced BOLD activity. NeuroImage 50, 1690–1701.

Menon, V., 2011. Large-scale brain networks and psychopathology: a unifying triple network model. Trends Cognit. Sci. 15, 483–506.
Miller, J.J., Fletcher, K., Kabat-Zinn, J., 1995. Three-year follow-up and clinical implications of a mindfulness meditation-based stress reduction intervention in the treatment of anxiety disorders. Gen. Hosp. Psychiatry 17, 192–200.
Monchi, O., Petrides, M., Petre, V., Worsley, K., Dagher, A., 2001. Wisconsin Card Sorting revisited: distinct neural circuits participating in different stages of the task identified by event-related functional magnetic resonance imaging. J. Neurosci. 21, 7733–7741.
Mooneyham, B.W., Mrazek, M.D., Mrazek, A.J., Schooler, J.W., 2016. Signal or noise: brain network interactions underlying the experience and training of mindfulness. Ann. N. Y. Acad. Sci. 1369, 240–256.
Morgan, D., 2003. Mindfulness-based Cognitive Therapy for Depression: A New Approach to Preventing Relapse. Taylor & Francis.
Noone, C., Hogan, M.J.J.B.p., 2018. A Randomised Active-Controlled Trial to Examine the Effects of an Online Mindfulness Intervention on Executive Control. In: Critical Thinking and Key Thinking Dispositions in a University Student Sample, vol. 6, p. 13.
Oldfield, R.C., 1971. The assessment and analysis of handedness: the Edinburgh inventory. Neuropsychologia 9, 97–113.
Patriat, R., Molloy, E.K., Meier, T.B., Kirk, G.R., Nair, V.A., Meyerand, M.E., Prabhakaran, V., Birn, R.M., 2013. The effect of resting condition on resting-state fMRI reliability and consistency: a comparison between resting with eyes open, closed, and fixated. Neuroimage 78, 463–473.
Pernet, C.R., Wilcox, R.R., Rousselet, G.A., 2013. Robust correlation analyses: False positive and power validation using a new open Source Matlab Toolbox. Front. Psychol. 3, 606.
Perronnet, L., Lecuyer, A., Mano, M., Bannier, E., Lotte, F., Clerc, M., Barillot, C., 2017. Unimodal versus bimodal EEG-fMRI neurofeedback of a motor imagery task. Front. Hum. Neurosci. 11, 193.
Peters, A.T., Burkhouse, K., Feldhaus, C.C., Langenecker, S.A., Jacobs, R.H., 2016. Aberrant resting-state functional connectivity in limbic and cognitive control networks relates to depressive rumination and mindfulness: a pilot study among adolescents with a history of depression. J. Affect. Disord. 200, 178–181.
Posner, M.I., Rothbart, M.K., Sheese, B.E., Tang, Y., 2007. The anterior cingulate gyrus and the mechanism of self-regulation. Cognit. Affect Behav. Neurosci. 7, 391–395.
Posse, S., Fitzgerald, D., Gao, K., Habel, U., Rosenberg, D., Moore, G.J., Schneider, F., 2003. Real-time fMRI of temporolimbic regions detects amygdala activation during single-trial self-induced sadness. Neuroimage 18, 760–768.
Power, J.D., Mitra, A., Laumann, T.O., Snyder, A.Z., Schlaggar, B.L., Petersen, S.E., 2014. Methods to detect, characterize, and remove motion artifact in resting state fMRI. Neuroimage 84, 320–341.
Raj, D., Anderson, A.W., Gore, J.C., 2001. Respiratory effects in human functional magnetic resonance imaging due to bulk susceptibility changes. Phys. Med. Biol. 46, 3331.
Rammstedt, B., John, O.P., 2007. Measuring personality in one minute or less: a 10-item short version of the Big Five Inventory in English and German. J. Res. Personal. 41, 203–212.
Ramot, M., Grossman, S., Friedman, D., Malach, R., 2016. Covert neurofeedback without awareness shapes cortical network spontaneous connectivity. Proc. Natl. Acad. Sci. U.S.A. 113, E2413–E2420.
Rance, M., Walsh, C., Sukhodolsky, D.G., Pittman, B., Qiu, M., Kichuk, S.A., Wasylink, S., Koller, W.N., Bloch, M., Gruner, P., 2018. Time course of clinical change following neurofeedback. Neuroimage 181, 807–813.
Ruiz, S., Buyukturkoglu, K., Rana, M., Birbaumer, N., Sitaram, R., 2014. Real-time fMRI brain computer interfaces: self-regulation of single brain regions to networks. Biol. Psychol. 95, 4–20.
Scharnowski, F., Veit, R., Zopf, R., Studer, P., Bock, S., Diedrichsen, J., Goebel, R., Mathiak, K., Birbaumer, N., Weiskopf, N., 2015. Manipulating motor performance and memory through real-time fMRI neurofeedback. J. Biol. Psychol. 108, 85–97.
Scheibner, H.J., Bogler, C., Gleich, T., Haynes, J.D., Bermpohl, F., 2017. Internal and external attention and the default mode network. Neuroimage 148, 381–389.
Seeley, W.W., Menon, V., Schatzberg, A.F., Keller, J., Glover, G.H., Kenna, H., Reiss, A.L., Greicius, M.D., 2007. Dissociable intrinsic connectivity networks for salience processing and executive control. J. Neurosci. 27, 2349–2356.
Shaurya Prakash, R., De Leon, A.A., Klatt, M., Malarkey, W., Patterson, B., 2012. Mindfulness disposition and default-mode network connectivity in older adults. Soc. Cognit. Affect Neurosci. 8, 112–117.
Sheline, Y.I., Barch, D.M., Price, J.L., Rundle, M.M., Vaishnavi, S.N., Snyder, A.Z., Mintun, M.A., Wang, S., Coalson, R.S., Raichle, M.E., 2009. The default mode network and self-referential processes in depression. Proc. Natl. Acad. Sci. Unit. States Am. 106, 1942–1947.
Sherwood, M.S., Kane, J.H., Weisend, M.P., Parker, J.G., 2016. Enhanced control of dorsolateral prefrontal cortex neurophysiology with real-time functional magnetic resonance imaging (rt-fMRI) neurofeedback training and working memory practice. Neuroimage 124, 214–223.
Shibata, K., Watanabe, T., Sasaki, Y., Kawato, M., 2011. Perceptual learning incepted by decoded fMRI neurofeedback without stimulus presentation. Science 334, 1413–1415.
Sitaram, R., Ros, T., Stoeckel, L., Haller, S., Scharnowski, F., Lewis-Peacock, J., Weiskopf, N., Blefari, M.L., Rana, M., Oblak, E., 2017. Closed-loop brain training: the science of neurofeedback. Nat. Rev. Neurosci. 18, 86.
Smith, E.E., Jonides, J., 1997. Working memory: a view from neuroimaging. Cogn. Psychol. 33, 5–42.
Song, X.W., Dong, Z.Y., Long, X.Y., Li, S.F., Zuo, X.N., Zhu, C.Z., He, Y., Yan, C.G., Zang, Y.F., 2011. REST: a toolkit for resting-state functional magnetic resonance imaging data processing. PLoS One 6, e25031.
Spitzer, R.L., Kroenke, K., Williams, J.B., Group, P.H.Q.P.C.S., 1999. Validation and utility of a self-report version of PRIME-MD: the PHQ primary care study. JAMA 282, 1737–1744.
Sridharan, D., Levitin, D.J., Menon, V., 2008. A critical role for the right fronto-insular cortex in switching between central-executive and default-mode networks. Proc. Natl. Acad. Sci. U. S. A. 105, 12569–12574.
Steyer, R., Schwenkmezger, P., Notz, P., Eid, M., 1994. Testtheoretische Analysen des Mehrdimensionalen Befindlichkeitsfragebogen (MDBF). Diagnostica 40 (4), 320–328.
Steyer, R., Schwenkmezger, P., Notz, P., Eid, M., 1997. Multidimensional Mood Questionnaire (MDMQ), vol. 33. Hogrefe, Göttingen.
Stoeckel, L., Garrison, K.A., Ghosh, S.S., Wighton, P., Hanlon, C.A., Gilman, J.M., Greer, S., Turk-Browne, N.B., Scheinost, D., Craddock, C., 2014. Optimizing real time fMRI neurofeedback for therapeutic discovery and development. Neuroimage: Clinical 5, 245–255.
Su, I.-W., Wu, F.-W., Liang, K.-C., Cheng, K.-Y., Hsieh, S.-T., Sun, W.-Z., Chou, T.-L., 2016. Pain perception can be modulated by mindfulness training: a resting-state fMRI study. Front. Hum. Neurosci. 10, 570.
Sulzer, J., Haller, S., Scharnowski, F., Weiskopf, N., Birbaumer, N., Blefari, M.L., Bruehl, A.B., Cohen, L.G., DeCharms, R.C., Gassert, R., Goebel, R., Herwig, U., LaConte, S., Linden, D., Luft, A., Seifritz, E., Sitaram, R., 2013a. Real-time fMRI neurofeedback: progress and challenges. Neuroimage 76, 386–399.
Sulzer, J., Sitaram, R., Blefari, M.L., Kollias, S., Birbaumer, N., Stephan, K.E., Luft, A., Gassert, R., 2013b. Neurofeedback-mediated self-regulation of the dopaminergic midbrain. Neuroimage 83, 817–825.
Tanay, G., Bernstein, A., 2013. State Mindfulness Scale (SMS): development and initial validation. Psychol. Assess. 25, 1286–1299.
Tang, Y.-Y., Hölzel, B.K., Posner, M.I., 2015. The neuroscience of mindfulness meditation. Nat. Rev. Neurosci. 16, 213–225.
Tang, Y.-Y., Ma, Y., Fan, Y., Feng, H., Wang, J., Feng, S., Lu, Q., Hu, B., Lin, Y., Li, J., 2009. Central and autonomic nervous system interaction is altered by short-term meditation. J. Auton. Nerv. Syst. 106, 8865–8870.
Taren, A.A., Gianaros, P.J., Greco, C.M., Lindsay, E.K., Fairgrieve, A., Brown, K.W., Rosen, R.K., Ferris, J.L., Julson, E., Marsland, A.L., 2017. Mindfulness meditation training and executive control network resting state functional connectivity: a randomized controlled trial. Psychosom. Med. 79, 674–683.
Terhune, D.B., Russo, S., Near, J., Stagg, C.J., Cohen Kadosh, R., 2014. GABA predicts time perception. J. Neurosci. 34, 4364–4370.
Thibault, R.T., MacPherson, A., Lifshitz, M., Roth, R.R., Raz, A., 2018. Neurofeedback with fMRI: a critical systematic review. Neuroimage 172, 786–807.
Touroutoglou, A., Lindquist, K.A., Dickerson, B.C., Barrett, L.F., 2015. Intrinsic connectivity in the human brain does not reveal networks for 'basic'emotions. Soc. Cognit. Affect Neurosci. 10, 1257–1265.
Tsuchimoto, S., Shibusawa, S., Mizuguchi, N., Kato, K., Ebata, H., Liu, M., Hanakawa, T., Ushiba, J., 2017. Resting-state fluctuations of EEG sensorimotor rhythm reflect BOLD activities in the pericentral areas: a simultaneous EEG-fMRI Study. Front. Hum. Neurosci. 11, 356.
Tung, K.C., Uh, J., Mao, D., Xu, F., Xiao, G., Lu, H., 2013. Alterations in resting functional connectivity due to recent motor task. Neuroimage 78, 316–324.
Uddin, L.Q., 2015. Salience processing and insular cortical function and dysfunction. Nat. Rev. Neurosci. 16, 55.
Uddin, L.Q., Supekar, K.S., Ryali, S., Menon, V., 2011. Dynamic reconfiguration of structural and functional connectivity across core neurocognitive brain networks with development. J. Neurosci. 31, 18578–18589.
Van Den Heuvel, M.P., Pol, H.E.H., 2010. Exploring the brain network: a review on resting-state fMRI functional connectivity. Eur. Neuropsychopharmacol. 20, 519–534.
Veit, R., Singh, V., Sitaram, R., Caria, A., Rauss, K., Birbaumer, N., 2012. Using real-time fMRI to learn voluntary regulation of the anterior insula in the presence of threat-related stimuli. Soc. Cognit. Affect Neurosci. 7, 623–634.
Verstynen, T.D., Deshpande, V., 2011. Using pulse oximetry to account for high and low frequency physiological artifacts in the BOLD signal. Neuroimage 55, 1633–1644.
Wang, Y.-Y., Li, X.-H., Zheng, W., Xu, Z.-Y., Ng, C.H., Ungvari, G.S., Yuan, Z., Xiang, Y.-T., 2018. Mindfulness-based interventions for major depressive disorder: a comprehensive meta-analysis of randomized controlled trials. J. Affect. Disord. 229 (15), 429–436.
Watanabe, T., Sasaki, Y., Shibata, K., Kawato, M., 2017. Advances in fMRI real-time neurofeedback. Trends Cognit. Sci. 21 (12), 997–1010.
Weick, K.E., Sutcliffe, K.M., Obstfeld, D., 2008. Organizing for high reliability: processes of collective mindfulness. In: Crisis Management, vol. 3, pp. 31–66.
Weiskopf, N., 2012. Real-time fMRI and its application to neurofeedback. Neuroimage 62, 682–692.
Weiskopf, N., Mathiak, K., Bock, S.W., Scharnowski, F., Veit, R., Grodd, W., Goebel, R., Birbaumer, N., 2004a. Principles of a brain-computer interface (BCI) based on real-time functional magnetic resonance imaging (fMRI). IEEE (Inst. Electr. Electron. Eng.) Trans. Biomed. Eng. 51, 966–970.
Weiskopf, N., Scharnowski, F., Veit, R., Goebel, R., Birbaumer, N., Mathiak, K., 2004b. Self-regulation of local brain activity using real-time functional magnetic resonance imaging (fMRI). J. Physiol. Paris 98, 357–373.
Weiskopf, N., Veit, R., Erb, M., Mathiak, K., Grodd, W., Goebel, R., Birbaumer, N., 2003. Physiological self-regulation of regional brain activity using real-time functional magnetic resonance imaging (fMRI): methodology and exemplary data. Neuroimage 19, 577–586.
Wells, R.E., Yeh, G.Y., Kerr, C.E., Wolkin, J., Davis, R.B., Tan, Y., Spaeth, R., Wall, R.B., Walsh, J., Kaptchuk, T.J., Press, D., Phillips, R.S., Kong, J., 2013. Meditation's impact

on default mode network and hippocampus in mild cognitive impairment: a pilot study. Neurosci. Lett. 556, 15–19.
Yarkoni, T., Poldrack, R.A., Nichols, T.E., Van Essen, D.C., Wager, T.D., 2011. Large-scale automated synthesis of human functional neuroimaging data. Nat. Methods 8, 665.
Yoo, S.-S., Fairneny, T., Chen, N.-K., Choo, S.-E., Panych, L.P., Park, H., Lee, S.-Y., Jolesz, F.A., 2004. Brain–computer interface using fMRI: spatial navigation by thoughts. Neuroreport 15, 1591–1595.
Yoo, S.S., Jolesz, F.A., 2002. Functional MRI for neurofeedback: feasibility study on a hand motor task. Neuroreport 13, 1377–1381.
Yoo, S.S., Lee, J.H., O'Leary, H., Lee, V., Choo, S.E., Jolesz, F.A., 2007. Functional magnetic resonance imaging-mediated learning of increased activity in auditory areas. Neuroreport 18, 1915–1920.
Yoo, S.S., Lee, J.H., O'Leary, H., Panych, L.P., Jolesz, F.A., 2008. Neurofeedback fMRI-mediated learning and consolidation of regional brain activation during motor imagery. Int. J. Imaging Syst. Technol. 18, 69–78.
Young, C.B., Raz, G., Everaerd, D., Beckmann, C.F., Tendolkar, I., Hendler, T., Fernández, G., Hermans, E.J., 2017. Dynamic shifts in large-scale brain network balance as a function of arousal. J. Neurosci. 37, 281–290.
Young, K.D., Zotev, V., Phillips, R., Misaki, M., Yuan, H., Drevets, W.C., Bodurka, J., 2014. Real-time FMRI neurofeedback training of amygdala activity in patients with major depressive disorder. PLoS One vol. 9, e88785.
Zeidan, F., Johnson, S.K., Diamond, B.J., David, Z., Goolkasian, P., 2010. Mindfulness meditation improves cognition: evidence of brief mental training. Conscious. Cognit. 19, 597–605.
Zotev, V., Krueger, F., Phillips, R., Alvarez, R.P., Simmons, W.K., Bellgowan, P., Drevets, W.C., Bodurka, J., 2011. Self-regulation of amygdala activation using real-time FMRI neurofeedback. PLoS One 6, e24522.
Zotev, V., Phillips, R., Yuan, H., Misaki, M., Bodurka, J., 2014. Self-regulation of human brain activity using simultaneous real-time fMRI and EEG neurofeedback. Neuroimage 85, 985–995.
Zuo, X.-N., Kelly, C., Adelstein, J.S., Klein, D.F., Castellanos, F.X., Milham, M.P.J.N., 2010. Reliable intrinsic connectivity networks: test–retest evaluation using ICA and dual regression approach, 49, 2163–2177.